Angewandte Chemie
Eine Zeitschrift der Gesellschaft Deutscher Chemiker

Supporting Information

Nanoscale Metal-Organic Layer Reprograms Cellular Metabolism to Enhance Photodynamic Therapy and Antitumor Immunity

*G. Lin, L. Tillman, T. Luo, X. Jiang, Y. Fan, G. Liu, W. Lin**

Supporting Information for

Nanoscale Metal-Organic Layer Reprograms Cellular Metabolism to Enhance Photodynamic Therapy and Antitumor Immunity

Gan Lin,[a],[b],† Langston Tillman,[c],† Taokun Luo,[a], Xiaomin Jiang,[a] Yingjie Fan,[a] Gang Liu,[b] Wenbin Lin,[a],[d],*

[a]Department of Chemistry, The University of Chicago, Chicago, IL 60637, USA
[b]State Key Laboratory of Molecular Vaccinology and Molecular Diagnostics & Center for Molecular Imaging and Translational Medicine, School of Public Health, Xiamen University, Xiamen 361102, China
[c]Pritzker School of Molecular Engineering, The University of Chicago, Chicago, IL 60637, USA
[d]Department of Radiation and Cellular Oncology and Ludwig Center for Metastasis Research, The University of Chicago, Chicago, IL 60637, USA

†These authors contributed equally.

*Corresponding author

Email: wenbinlin@uchicago.edu

1. Experiment Section

1.1. Chemicals and methods

Chemicals and assay kits were purchased from Sigma-Aldrich, Cayman Chemical and Thermo Fisher Scientific (USA) and used as received unless otherwise specified. Transmission electron microscopy (TEM) was conducted on a TECNAI Spirit TEM. Powder X-ray diffraction (PXRD) patterns were performed on a Bruker D8 Venture diffractometer using a Cu Kα radiation source (λ 1.54178 Å); the obtained results were processed with PowderX software. Dynamic light scattering (DLS) and zeta potential measurements were carried out on a Zetasizer Nano ZS instrument (Malvern Instruments, Malvern, UK). Inductively coupled plasma-mass spectrometry (ICP-MS) was conducted on an Agilent 7700x ICP-MS and the obtained results were analyzed using ICP-MS Mass Hunter version 4.6 C.01.06. Ultraviolet−visible (UV−vis) spectroscopy was performed on a Shimadzu UV-2600 spectrophotometer. ^{1}H and ^{19}F NMR spectra of digested samples were conducted on an NMR 400 DRX spectrometer (Bruker) at 400 MHz. The fluorescence intensity of 2', 7' –dichlorofluorescein (DCF) was recorded in a Synergy HTX plate reader (Agilent Technologies).

PBS was purchased from ThermoFisher Scientific. RPMI-1640 medium was purchased from Corning. Fetal bovine serum (FBS) was purchased from VWR (USA). 3-(4,5- dimethylthiazol-2-yl)-5-(3-carboxy-methoxyphenyl)-2-(4-sulfo-phenyl)2H-tetrazolium (MTS) was provided by Promega (USA). Murine triple negative breast cancer cell line 4T1, murine colorectal carcinoma CT26 cells, Trypsin-EDTA solutions were purchased from the American Type Culture Collection (ATCC, Rockville, MD). Flow cytometry experiments were conducted on an LSR-Fortessa 4-15 (BD Biosciences, USA) and analyzed by using FlowJo software (Tree Star, USA). Confocal laser scanning microscopy (CLSM) images were acquired on a Leica SP8 microscope. Fluorescence lifetime imaging was conducted on a Leica Stellaris 8 laser scanning confocal microscope. CLSM imaging studies were performed in the

Integrated Light Microscopy Facility at the University of Chicago, and the acquired images were analyzed using ImageJ software (NIH, USA).

CT26 and 4T1 cells were cultured in RPMI-1640 medium and supplemented with 10% FBS and 1% Penicillin-Streptomycin (Cytiva, USA). CT26 and 4T1 cells were kept in an incubator (100% humidity, and 5% CO_2) at 37°C. BALB/c breeders were purchased from Charles River Laboratories (USA) and bred at the animal facility at the University of Chicago. 6-8 weeks aged BALB/c mice were used for animal studies. The study protocol (ACUP 72408) was reviewed and approved by the Institutional Animal Care and Use Committee (IACUC) at the University of Chicago [D16-00322 (A3523-01)]. The histology related services in this study were carried out by the Human Tissue Resource Center at the University of Chicago. Histological slides were scanned on an Olympus Scanner under a 40x whole slide scanner in the Integrated Light Microscopy Core at the University of Chicago, and the images were analyzed by the QuPath-0.2.3 software.

1.2. Synthesis and characterization of Hf-DBP MOL and BrP@MOL

Synthesis of PA-capped Hf-DBP MOL

Hf-DBP MOL was synthesized by following our previous publication.[1] Briefly, 2 mg $HfCl_4$, 1 mg H_2DBP, 8.5 μL propionic acid (PA), 5 μL H_2O and 1 mL DMF were added to a 1-dram glass vial. The vial was placed in an 80 °C oven for 24 h. After cooling to room temperature, the resultant purple solid was collected by centrifugation, washed twice with DMF and ethanol, and stored as an ethanol dispersion in the dark.

Synthesis of TFA-modified Hf-DBP MOL

To lower the polarity of solvent, ethanolic suspensions of PA-capped Hf-DBP were washed sequentially with acetonitrile twice and benzene twice. 10 mL of PA-capped Hf-DBP dispersion (2 mM based on DBP) and 10-fold excess of trimethylsilyl trifluoroacetate (TFA-TMS) were mixed in benzene in a vial. The mixture was stirred for 12 hours under an N_2 atmosphere. The suspensions were washed with acetonitrile and EtOH sequentially and stored as ethanol dispersions for further use.

Synthesis of BrP@Hf-DBP MOL

To a 1-dram glass vial, 1.0 mL of ethanolic solution containing TFA-modified Hf-DBP MOL (2 mM based on DBP) and 3-bromopyruvate (BrP, 20 mM) was added. The mixture was stirred at room temperature overnight. The resulting solid was collected by centrifugation and washed twice with ethanol, and stored as an ethanol dispersion.

NMR analysis of the digested MOL

Approximately 0.5 mg of PA-capped Hf-DBP, TFA-modified Hf-DBP, or BrP@Hf-DBP was dried under vacuum. A mixture of 500 μL DMSO-d_6, 50 μL D_3PO_4 and 50 μL D_2O was added to the dried MOL, followed by 10 min sonication to afford a homogeneous solution. The obtained solution was subject to ^1H and ^{19}F NMR analyses.

Determination of BrP loading and DBP in BrP@MOL

The loading of BrP in BrP@MOL was determined by dividing the integral of BrP by that of DBP in ^1H NMR spectrum of the digested sample. To determine the concentration of DBP, BrP@MOL (10 μL) was digested using a mixture of 940 μL DMSO and 50 μL H_3PO_4. The concentration of DBP was determined by UV-vis absorption at the characteristic Soret band at 409 nm. Hf concentration was determined by ICP-MS. The BrP: DBP: Hf_{12} SBU ratio was calculated as 0.81: 1: 2, which yielded the formula $Hf_{12}(\mu_3$-

$O)_8(\mu_3\text{-}OH)_8(\mu_2\text{-}OH)_6(DBP)_6(\mu_2\text{-}BrP)_{4.86}(\mu_2\text{-}TFA)_{1.14}$.

Release profiles of BrP

The concentration of BrP was quantified with LC-MS on an Agilent 6540 Q-T of MS-MS with 1290 UHPLC (5μm Agilent C_{18} reverse phase column). BrP@MOL was prepared and redispersed in the same volume of 1× PBS and 0.1× PBS in 1.5 mL Eppendorf tubes (n=3), respectively. The ep tubes were centrifuged for 10 minutes at 14000 rpm after 10 minutes, 20 minutes, 30 minutes, 1h, 2h, 4h, 12h, 24h, and 48h incubation at room temperature. The supernatants were collected and derivatized as previously reported.[2] The resulting derivatized supernatants were directly measured by LC-MS. The release percentages were fitted by the Hill function in GraphPad Prism software.

1.3. DLS and zeta-potential measurements

Dynamic light scattering (DLS) and zeta-potential measurements were performed on TFA-modified Hf-DBP MOL and BrP@MOL. 1 mL MOL or BrP@MOL aqueous dispersion at a DBP concentration of 5 μM was added to the cell for DLS and ζ potential measurements.

1.4. Reactive oxygen species (ROS) generation in test tubes

2', 7' –Dichlorofluorescein (DCF) assays were used to measure time-dependent reactive oxygen species (ROS) generation of MOL and BrP@MOL upon light illumination (630 nm). Briefly, the hydrolytic process of DCFH-DA was carried out by adding 2 mL NaOH (10 mM) aqueous solution to 0.5 mL DCFH-DA (1 mM) DMSO solution, followed by vigorous stirring for 30 min in the dark. 10 mL PBS (25 mM, pH 7.4) was added to stop the hydrolytic process to obtain the DCFH solution. The freshly-prepared DCFH was mixed with MOL or BrP@MOL suspension to afford the aqueous dispersions with equivalent concentrations of 5 μM DBP and 10 μM DCF. The solutions were then exposed to light irradiation (630 nm, 80 mW/cm^2) for 0, 1, 2.5, 5 minutes. At each time point, the fluorescence intensity of DCF was measured using a fluorescence plate reader (λ_{ex} = 485, λ_{em} = 520 nm).

1.5. Cell viability assays

The light irradiated [denoted as (+)] and dark [denoted as (-)] cytotoxicities of MOL and BrP@MOL were assessed on CT26 and 4T1 cells using 3-(4,5- dimethylthiazol-2-yl)-5-(3-carboxymethoxyphenyl)-2-(4-sulfo-phenyl)-2H-tetrazolium (MTS) assay (Promega, USA). CT26 or 4T1 cells were seeded in 96-well plates (density: 2000 cells/well) and cultured overnight. MOL or BrP@nMOL was added to the wells at equivalent DBP concentrations of 0, 0.156, 0.312, 0.625, 1.25, 2.5, 5, 10, 20 μM and incubated for 6 hours (n = 3), followed by light irradiation (630 nm, 80 mW/cm^2) for 10 minutes. Cells were further incubated for 48 hours and the viability was determined by MTS assay. IC50 values were determined by fitting cell viabilities with the dose response curves in Origin Lab.

1.6. Synergistic effects

To determine whether there is a synergistic effect in the combination of BrP@MOL-mediated metabolic reprogramming and PDT, cell viability after the combination treatment [i.e., BrP@MOL(+)] was compared with a purely additive result from BrP@MOL(-) and MOL(+). The additive index was calculated using the following relationship:

$f_{additive}=f_{MOL(+)}\times f_{BrP@MOL(-)}$,

$f_{MOL(+)}$ and $f_{BrP@MOL(-)}$ are the fractions of surviving cells in MOL(+) and BrP@MOL(-) groups.

$f_{combination}$ is the fraction of surviving cells in BrP@MOL(+) group. If $f_{additive} > f_{combination}$, there is a synergistic effect. If $f_{additive} = f_{combination}$, there is an additive effect. If $f_{additive} < f_{combination}$, antagonistic effect.

1.7. Cellular uptake

The relative cellular uptake of MOL and BrP@MOL was evaluated on CT26 cells. Cells were seeded in 6-well plates (density: 2×10^5 cells/well) and cultured in RPMI medium containing 10% FBS overnight. MOL or BrP@MOL was added to each well at an equivalent DBP concentration of 5 μM and incubated for 6 h. The medium was removed, and cells were washed with PBS twice, trypsinized, and subjected to flow cytometry analysis. The relative cellular uptake of MOL and BrP@MOL was monitored by measuring the fluorescence intensity of DBP using the channel of Brilliant Violet 660 (excitation 405 nm / emission 645 nm).

Time-dependent cellular uptake of MOL or BrP@MOL was evaluated on CT26 cells by UV-Vis spectroscopy. Cells were seeded on 6-well plates (density: 5×10^5/well) and cultured in RPMI medium containing 10% FBS overnight. MOL or BrP@MOL was added to each well with a final equivalent DBP concentration of 10 μM (n = 3). At different time points (i.e., 1, 2, 4, 8 hr), the medium was discarded and the cells were washed twice with PBS, trypsinized and collected by centrifugation (1800 rpm, 5 min). After counting in a hemocytometer, cells were digested with 1 mL of DMSO (10% H_3PO_4) in 2 mL Eppendorf tubes. During a 48-hour period, the cells were treated with strong sonication every 12 hours. The DBP concentration of each sample was determined by UV-Vis absorbance at 409 nm according to the standard curve.

1.8. Intracellular ROS generation

The intracellular ROS generation was detected in CT26 cells after different treatments by using flow cytometry and CLSM. For flow cytometry studies, CT26 cells were seeded in 6-well plates at a density of 2×10^5 cells/well and cultured overnight. MOL, BrP@MOL, or BrP was added to the dishes at an equivalent DBP concentration of 2.5 μM (or BrP concentration of 2.02 μM). After 6 h incubation, DCF-DA (final concentration: 20 μM) was added to each well and further incubated for 30 minutes. The cells were illuminated with light (630 nm, 80 mW/cm^2, 10 mins), and washed with PBS twice. The cells were then trypsinized and collected for flow cytometry analysis. The cells in dark control groups were treated in the same way, except without light irradiation. For CLSM experiments, CT26 cells were seeded in 35 mm glass bottom dishes at a density of 2×10^5 cells/dish and cultured overnight. The cells were treated using the same way in flow cytometry experiments, but not detached. The medium was removed, and the cells were washed with PBS twice and refreshed with RPMI-1640 medium and imaged immediately under a Leica SP8 microscope.

1.9. Mitochondria membrane potential

The mitochondrial membrane potential was evaluated on CT26 cells by using JC-1 mitochondrial potential sensors (Invitrogen™) under CLSM. CT26 cells were seeded on 35 mm glass bottom dishes at a density of 2×10^5 cells/dish and cultured overnight. MOL, BrP@MOL, or BrP was added to the dishes at an equivalent DBP concentration of 2.5 μM (or BrP concentration of 2.02 μM). After 6 h incubation, the cells in the irradiated groups were illuminated with light (630 nm, 80 mW/cm^2, 10 mins). JC-1 sensors were immediately added to the dishes at a final concentration of 10 μM. After 30 min incubation, the cells were washed with cold PBS and added with RPMI-1640 medium, and imaged under a Leica SP8 microscope.

1.10. Apoptosis analysis

The apoptosis of CT26 cells after different treatments was evaluated by flow cytometry and CLSM. CT26 cells were seeded in 6-well plates at a density of 2 × 105 cells/well and cultured overnight. MOL, BrP@MOL, or BrP was added into the dishes at an equivalent DBP concentration of 2.5 μM (or BrP concentration of 2.02 μM) and incubated for 6 h. The cells in the irradiated groups were illuminated with light (630 nm, 80 mW/cm^2, 10 mins). The cells were further cultured in the 37 ℃ incubator for another 24 h. The cells were washed with cold PBS, trypsinized and stained with Alexa Fluor 488 labeled Annexin V (1:20 dilution) and propidium iodide (PI, 1 μg/mL) in 1x Annexin V binding buffer following the vendor's protocol for flow cytometry. For CLSM analysis, CT26 cells were seeded in 35 mm glass bottom dishes at a density of 2 × 10^5 cells/well and cultured overnight. The cells were treated and stained in the same way with flow cytometry, except the addition of a staining step with Hoechst 33342 (3 μg/mL, 5 min at RT). The dishes were then added with 1 mL 1x Annexin V binding buffer and imaged under a Leica SP8 microscope.

1.11. Immunogenic cell death of cancer cells

Immunogenic cell death (ICD) was evaluated by detecting the expression of Calreticulin (CRT) on CT26 cells using flow cytometry and CLSM. For flow cytometry studies, CT26 cells were seeded in 6-well plates at a density of 2 × 10^5 cells/well and cultured overnight. MOL, BrP@MOL, or BrP was added to the dishes at an equivalent DBP concentration of 2.5 μM (or BrP concentration of 2.02 μM). After 6 h incubation, the cells in the irradiated groups were illuminated with light (630 nm, 80 mW/cm^2, 10 mins). After a further 24 h incubation, the medium was removed, and the cells were washed with PBS and trypsinized to obtain cell suspensions. The cells were stained with Alexa Fluor 488 labelled anti-Calreticulin Antibodies (1:150 dilution) in 1% BSA PBS solution on ice for 30 min. The cells were then washed with PBS and resuspended in FACS buffer for flow cytometry.

For CLSM experiments, CT26 cells were seeded in 35 mm glass bottom dishes at a density of 2 × 10^5 cells/dish and cultured overnight, and were then treated in the same way in flow cytometry studies. At 24 h post the treatment, the cells were fixed in methanol (-20 ℃) for 10 min, and blocked with 3% BSA and 1% FBS at RT for 1h. The cells were then stained with Alexa Fluor 488 labelled anti-Calreticulin Antibodies (1:150 dilution) in 1% BSA PBS at RT for 1 hour. After staining with Hoechst (3 μg/mL) for 10 min, the cells were washed with PBS twice and mounted for CLSM images under a Leica SP8 microscope.

CT26 cells were seeded in a 96-well plate at a density of 7500 cells/well overnight in FBS-free RPMI 1640. MOL, 3-BrP, and BrP@MOL were respectively added to wells to yield concentrations of 5μM DBP-equivalent for the MOL and BrP@MOL groups and a BrP concentration of 4μM for the BrP groups. The cells were incubated at 37 ℃ for 8 hours, after which half of each group underwent light irradiation (630 nM, 100mW/cm^2, 10 mins, 60J/cm^2 in total). The cells were further incubated for 24 hours. After incubation, the plates were centrifuged (300g, 5min), and the supernatant was collected. The extracellular ATP concentration was determined by an ATP Bioluminescence Assay (Fischer Scientific). The HMGB1 concentration was determined by an HMGB1 ELISA Assay (Chondrex).

1.12. Fluorescence lifetime imaging

CT26 cells were seeded in 35 mm glass bottom dishes at a density of 2 × 105 cells/well and cultured overnight. MOL or BrP@MOL was added into the dishes at an equivalent DBP concentration of 2.5 μM. After 12 h incubation, fluorescence lifetime images (FLIM) of CT26 cells were measured under a Leica

Stellaris 8 FALCON FLIM microscope, with FAD being excited at 451 nm and emitting at 500-600 nm. The fluorescence of FAD in the cells was measured under a 63× objective lens. The fluorescence lifetime image of FAD and the ratio of free- to protein-bound FAD (a2/a1 ratio) were analyzed by fitting the acquired FAD fluorescence images with two-exponential re-convolution in LAX_X_FLIM software.

1.13. In vitro intracellular oxygen sensing

CT26 cells were seeded in 35 mm glass bottom dishes at a density of 2.5×10^5 cells/well and cultured in a hypoxia chamber overnight ($pO_2 = 0.05$). $Ru(dpp)_3(Cl)_2$ was added to the dishes at a concentration of 10 μg/mL. Additionally, MOL or BrP@MOL was added to the relevant dishes at an equivalent DBP concentration of 15 μM and BrP was added to the relevant dish at an equivalent of 12 μM. After co-incubating in the hypoxia chamber for another 6 hours, the cells were stained with Hoechst 33342 (1:1000) in PBS for 3 minutes. After washing with PBS, the dishes were observed on a Leica SP8 confocal microscope. The data were analyzed with Fiji ImageJ (NIH).

1.14. In vitro GAPDH and LDH activity

CT26 cells were seeded in 12-wells at a density of 10000 cells/well. MOL or BrP@MOL was added into the well at an equivalent DBP concentrations of 10 μM. After 24 h or 48 h incubation, the medium was removed, and the cells were washed with PBS. The cells were collected and lysed using RIPA buffer. The GAPDH and LDH activity was determined by GAPDH Activity Assay Kit (Sigma-Aldrich, MAK277) and LDH Assay Kit (Thermo fisher scientific, C20300), respectively, by following the vendor's protocols. The values for different groups were normalized by cell numbers and then compared, with PBS serving as the control.

1.15. In vitro Lactate and ATP measurements

CT26 cells were seeded in 96-wells at a density of 2000 cells/well. MOL or BrP@MOL was added to the wells at an equivalent DBP concentrations of 10 μM. After 24 h or 48 h incubation, the medium was removed, and the cells were washed with PBS. The cells were collected and lysed using RIPA buffer. The intracellular ATP and lactate levels were determined using ATP determination kit (Thermo fisher scientific, 1967043) and L-Lactate Assay Kit (Cayman Chemical, 700510), respectively, by following the vendor's protocols. The values for different groups were normalized by cell numbers and then compared, with PBS serving as the control.

1.16. In vivo anti-cancer efficacy

In vivo efficacy of different treatments was tested on subcutaneous CT26 and orthotopic 4T1 tumor models. BALB/c mice were subcutaneously injected with 2×10^6 cells/mouse in the right flanks (for CT26) or 1×10^6 cells/mouse into the 2rd mammary pads of female mice (for 4T1) on day 0. When tumor volume reached around 80 mm^3 at day 7, mice were randomized into several groups (n=5). PBS, MOL, BrP, or BrP@MOL was injected intratumorally at an equivalent DBP dose of 0.2 μmol (or BrP concentration of 0.162 μmol) on day 7 and 9. 8 hours later, the mice were anaesthetized with 1.5% (V/V) isoflurane/O_2. The body of each mouse was covered with black cloth and the tumor area was illuminated with light (630 nm, 80 mW/cm^2) for 15 mins. After light illumination, anti-PD-L1 antibody (100μg/mouse) was given immediately by intraperitoneal injection. Tumor volumes and body weights were monitored daily; the volume = length×$width^2$/2. On day 19 (or 23), the mice were sacrificed, and the tumors were excised, weighed, photographed and sectioned for hematoxylin and eosin (H&E) staining and terminal deoxynucleotidyl transferase dUTP nick end labeling (TUNEL) staining. Major organs were harvested and sectioned for H&E staining.

1.17. In vivo GAPDH activity, lactate measurement and hypoxia

CT26 tumors were subcutaneously injected with 2×10^6 cells/mouse in the right flanks on day 0. PBS, MOL, or BrP@MOL was injected intratumorally with an equivalent DBP dose of 0.2 μmol (or BrP concentration of 0.162 μmol) on day 7 and 9 (n=4). On day 10, tumor tissues were harvested and a fixed quantity (20 mg) of tumor tissue were homogenized in 2 mL of lysate buffer. The GAPDH activity and lactate levels were measured by using GAPDH Activity Assay Kit (Sigma-Aldrich, MAK277) and L-Lactate Assay Kit (Cayman Chemical, 700510), respectively, by following the vendor's protocols.

The hypoxia of tumor tissues was evaluated by immunofluorescence assay. The tumors were excised and frozen with optimal cutting temperature (OCT) compound at -80 °C for 12 h. The blocks were sectioned, fixed with the mixture of 75% acetone and 25% ethanol at -20 °C for 10 minutes, and washed with Tris-buffered saline with 0.1% Tween-20 (TBST) to remove OCT. The sections were blocked by 5% FBS in PBS, then incubated with carbonic anhydrase 9 (CA9) primary antibody (1:100 dilution) in 0.5% BSA in PBS for 45 min. After washing with TBST, the sections were incubated with fluorophore conjugated secondary antibody (1:500 dilution) for 1 hour. The sections were washed with TBST and incubated with Hoechst (1: 3000 dilution) in PBS for 10 mins. The sections were washed with TBST and water, and observed under a Leica SP8 confocal microscope.

1.18. Immune cell profiling

CT26 tumor-bearing BALB/c mice (n = 4) were inoculated and treated in the same way as in anti-cancer efficacy study. On day 14, and the tumors and tumor-draining lymph nodes (TDLNs) were harvested, digested for immune cell profiling by flow cytometric analysis. Briefly, the harvested tumors and TDLNs were digested in 37 °C by 0.6 mL of RPMI-1640 medium (containing 10% FBS, 1 mg/mL collagenase I, 250 μg/mL collagenase IV and 50 μg/mL DNase I) for 45 mins. The digests were neutralized with 5 mL RPMI-1640 medium and gently ground. After being filtered through a sterile cell strainer (40 μm, Corning), cells pellets were collected by centrifugation (300 g, 5 min) at 4 °C. 2 mL of ACK buffer (ThermoFisher Scientific) was added into the tube to lyse red blood cells. The remaining cells were centrifugated (300 g, 5 min) at 4 °C, and washed with ice-cold FACS buffer, and first stained with LIVE/DEAD™ fixable yellow dead cell stain kit (1: 1000 dilution). The cells were then washed with FACS buffer, and stained with several fluorochrome-conjugated rat anti-mouse antibodies 1:100 at 4 °C for 45 minutes. The information of antibodies, e.g., conjugated dyes, vendor and clone numbers, is listed as follows: CD45-BV421 (Biolegend, 30-F11), CD11b-SB600 (Invitrogen, 2492201), CD11c-PE/eFluor 610 (Invitrogen, 2459633), MHCII-PE/Cy7 (Invitrogen, 2450622), CD80-FITC (Biolegend, 16-10A1), CD86-PE (Invitrogen, 2430472), CD3e-SB600 (Invitrogen, 2403315), CD8-APC/efluor 780 (Invitrogen, 2417685), CD4-Alexa Fuor 488 (Invitrogem, 2492208), PD-L1-APC (Biolegend, 124312). The cells were centrifugated (300 g, 5 min) at 4 °C, washed and resuspended in FACS buffer for flow cytometry. Representative gating strategies are shown in Figure S27 and Figure S28.

1.19. Tumor re-challenging studies

The immune memory effect was evaluated by tumor re-challenging studies. CT26 tumor-bearing BALB/c mice were inoculated and treated with BrP@MOL(+) in the same way in anti-cancer efficacy study. Four out of ten mice were cured. On day 30 after the first CT26 inoculation, these cured (tumor-free) BALB/c mice treated by BrP@MOL(+) and the cured mice from BrP@MOL(+) plus α PD-L1 group were re-inoculated with 2×10^6 CT26 cells in the left flanks subcutaneously. Naive mice were inoculated in the same way and served as control. The tumor volumes were recorded every 2 days.

1.20. Tumor retention studies

24 BALB/c mice were subcutaneously inoculated with $2x10^6$ CT26 cells on the right flank on day 0. When the tumors grew to a volume of $100mm^3$ around day 7, the mice were randomized for treatment. The mice were each intratumorally injected with BrP@MOL (DBP equivalent dose of 0.2 μmol). The mice were then sacrificed at 5min, 1 hr, 4 hr, 24 hr, 48 hr, and 1 week after the injection (n=4). The whole tumors were excised and digested with 70% trace-metal-free HNO_3. The Hf content was determined by ICP-MS. The Hf content in the whole tumor is presented below as a % of the initial Hf content and errors as ±SEM. The data demonstrates an average drug retention rate of 50.8% a week after the initial injection.

1.21. RNA-seq studies

Six BALB/c mice were subcutaneously inoculated with $2x10^6$ CT26 cells on the right flank on day 0. When the tumors grew to a volume of $100mm^3$ around day 7, the mice were randomized for treatment. Three mice were intratumorally injected with PBS for a control group and three were intratumorally injected with BrP @ MOL (DBP equivalent dose of 0.2μmol) for two treatment groups. After eight hours, the mice in the treatment group were treated with PDT (630nM, $80mW/cm^2$) for 15 minutes. Seven days after treatment, the mice were sacrificed, and the tumors were excised for analysis. The tumors were digested using a mixture of 1 mg/ml collagenase I (Sigma-Aldrich) and 0.25 mg/ml collagenase IV (Sigma-Aldrich) at 37 °C for 30 min. The RNA was extracted with Trizol according to the nanoString user manual and RNA-seq was done by the University of Chicago human immunologic monitoring facility with a nanoString nCounter Tumor Signaling 360 Panel. Information about relevant genes was obtained through the Mouse Gene Database (The Jackson Laboratory). Data were analyzed by ROSALIND® (https://rosalind.bio/), with a HyperScale architecture developed by ROSALIND, Inc. Normalization, fold changes, and p-values were calculated using criteria provided by NanoString (https://nanostring.com). ROSALIND® follows the nCounter® Advanced Analysis protocol of dividing counts within a lane by the geometric mean of the normalizer probes from the same lane. Housekeeping probes to be used for normalization are selected based on the geNorm algorithm as implemented in the NormqPCR R library. The abundance of various cell populations is calculated on ROSALIND using the Nanostring Cell Type Profiling Module. ROSALIND performs a filtering of Cell Type Profiling results to include results that have scores with a p-Value greater than or equal to 0.05. P-value adjustment is performed using the Benjamini-Hochberg method of estimating false discovery rates (FDR). Enrichment was calculated relative to a set of background genes relevant to the experiment. We generally see upregulation of genes associated with cell apoptosis in the treated condition and upregulation of survival genes in the PBS group. We also see an increase in genes regulating an immune response in the PBS group, suggesting a dampened immune system influence in the tumor site. Additionally, the prevalence of the JNK/MAPK signaling gene expression reveals a potential autophagic route of cell death.

Between PBS and BrP@MOL(+)-treated tumors, 20 genes passed the threshold of the nCounter PanCancer Immune Profiling Panel with ≥1.5-fold expression changes and adjacent p values less than 0.05. Compared to the PBS group, the BrP@MOL(+) group induced apoptosis pathways in the tumors, demonstrated by upregulation of thrombospondin 1 (*Thbs1*), PDZ and LIM domain 5 (*Pdlim5*), heme oxygenase 1 (*Hmox1*), and downregulation of breast cancer 1 (*Brca1*), *Cd38*, and colony stimulating factor 1 receptor (*Csf1r*), as well as interfering cell proliferation by upregulating dyskeratosis congenita 1 (*Dkc1*) and oncostatin M receptor (*Osmr*) Importantly, BrP@MOL(+) altered the metabolism

environment by upregulating lipocalin 2 (*Lcn2*) and downregulating pyruvate dehydrogenase kinase, isoenzyme 1 (*Pdk1*). BrP@MOL(+) treatment also enhanced the immune cell infiltration, shown by upregulation of arginase (Arg1) and downregulation of granzyme A (*Gzma*). The immune response was also regulated by BrP@MOL(+), which downregulated histocompatibility 2, class II antigen A, alpha (*H2-Aa*) and histocompatibility 2, class II antigen A, beta 1(*H2-Ab1*), circadian locomotor output cycles kaput (*Clock*), Fibroblast growth factor receptor 1 (*Fgfr1*), AT-Rich Interaction Domain 4A (*Arid4a*), Protein tyrosine phosphatase, receptor type, C (*Ptprc*). In all, BrP@MOL(+) showed significant metabolism alteration, induced strong tumor apoptosis, and regulated antitumor immunity.

1.22. Statistical analysis

Data are presented as mean ± standard deviation (SD). Statistical analysis was performed on Origin Lab software using One-way Repeated Measures ANOVA method with Tukey's honest significance test. Statistical significance is represented as *P < 0.05, **P < 0.01, and ***P < 0.001.

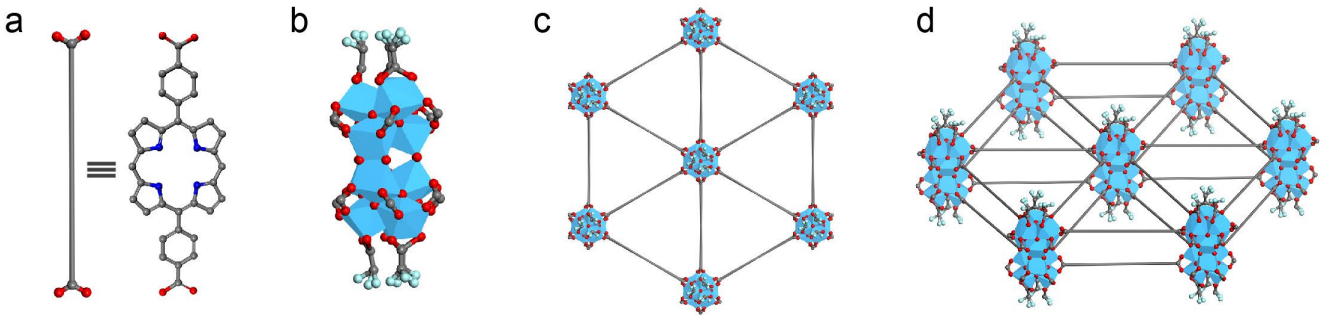

Figure S1. Structure models of TFA-modified Hf-DBP MOL. (a) Simplified and full structure model of H_2DBP ligand. (b) The structure of mono-substituted $Hf_{12}(\mu_3\text{-}O)_8(\mu_3\text{-}OH)_8(\mu_2\text{-}OH)_6(RCO_2)_{12}(TFA)_6$ SBU; RCO_2 represents the carboxylate group of H_2DBP ligand. (c) *c* axis view of the MOL showing the mono-layer structure. (d) Side view of the MOL indicating the locations of the bridging ligands of H_2DBP within the mono-layer framework (sky blue: Hf, pale light blue: F, red: O, grey: C; H atoms are omitted for clarity).

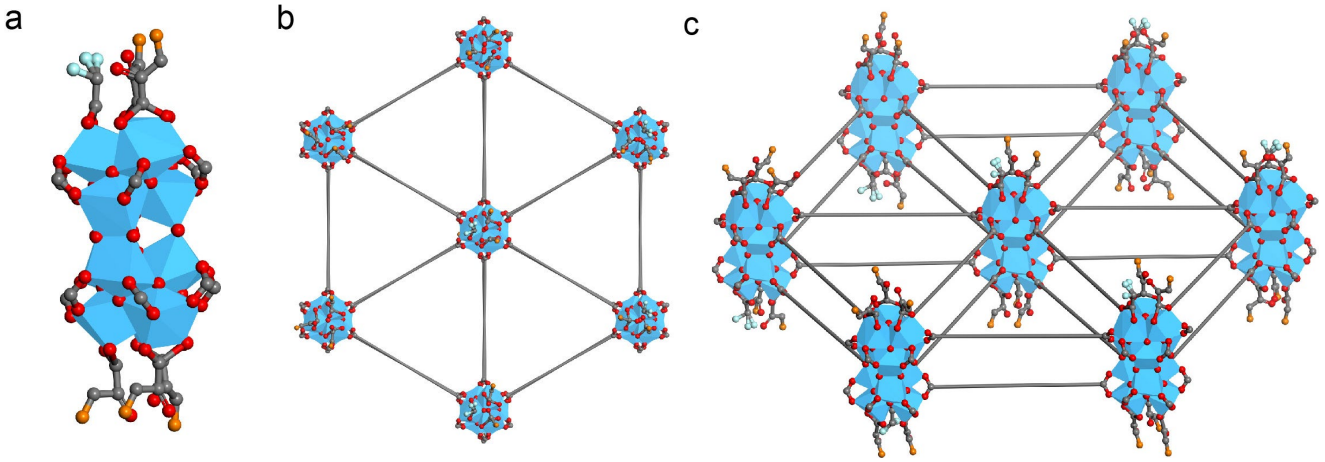

Figure S2. Structure models of BrP@MOL. (a) The structure of mono-substituted $Hf_{12}(\mu_3\text{-}O)_8(\mu_3\text{-}OH)_8(\mu_2\text{-}OH)_6(DBP)_6(\mu_2\text{-}BrP)_{4.86}(\mu_2\text{-}TFA)_{1.14}$ SBU; RCO_2 represents the carboxylate group of DBP ligand. (b) Top view of BrP@MOL showing its monolayer structure. (c) Side view of BrP@MOL showing SBU-anchored BrP (sky blue: Hf, pale light blue: F, red: O, Br: orange, grey: C).

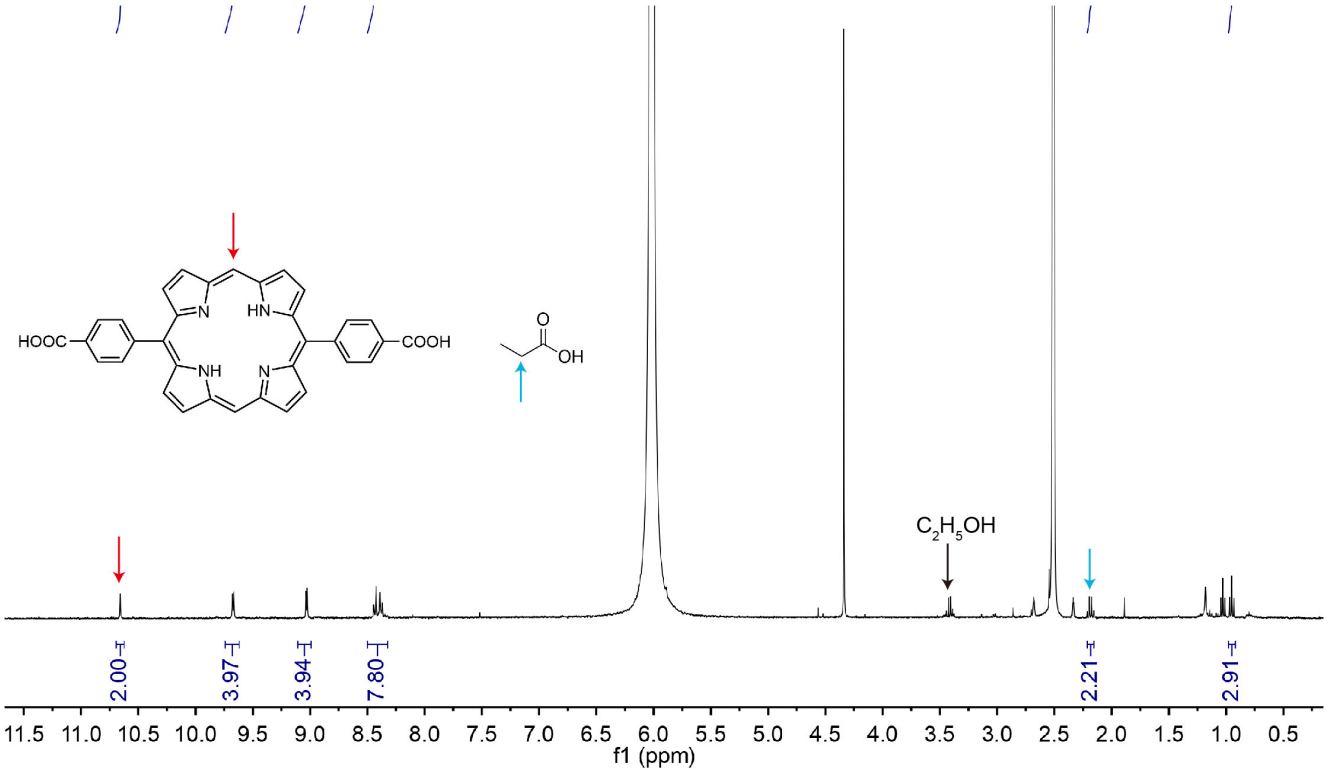

Figure S3. ^{1}H NMR digested PA-capped Hf-DBP MOL.

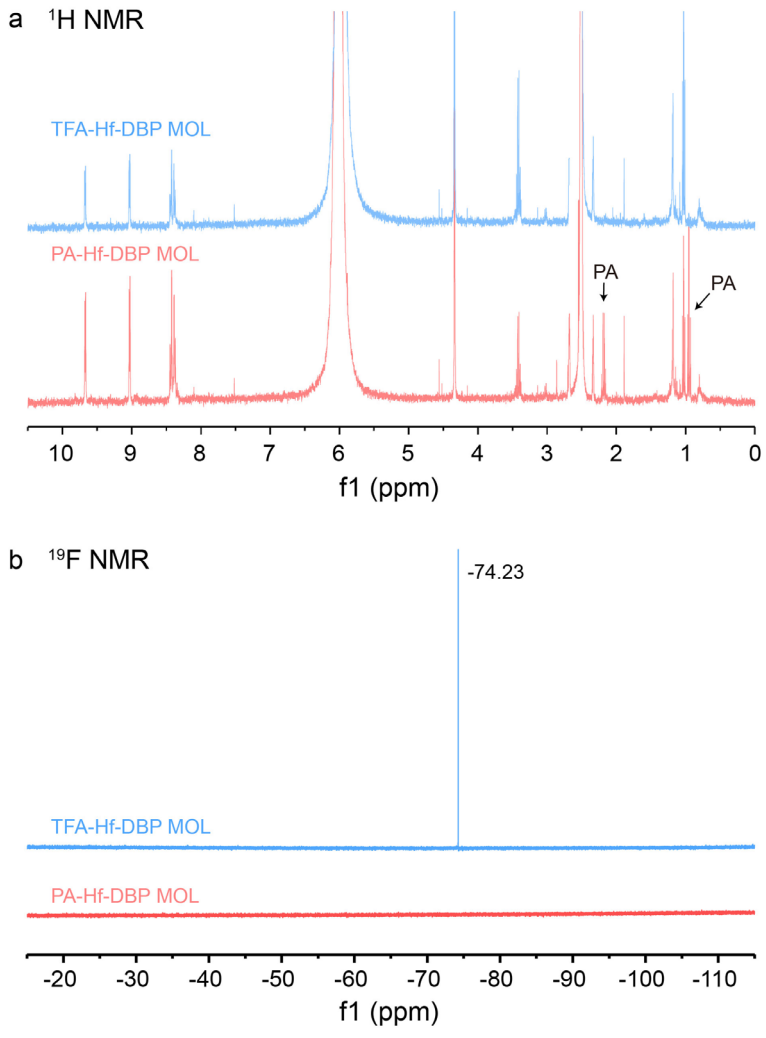

Figure S4. ^{1}H NMR (a) and ^{19}F NMR (b) spectrum of digested PA tapped Hf-DBP MOL and TFA modified Hf- DBP MOL. Digested TFA modified MOL in DMSO-d_6 shows the disappearance of PA signal in the ^{1}H NMR and the emergence of TFA in the ^{19}F NMR spectrum, suggesting PA was replaced by TFA.

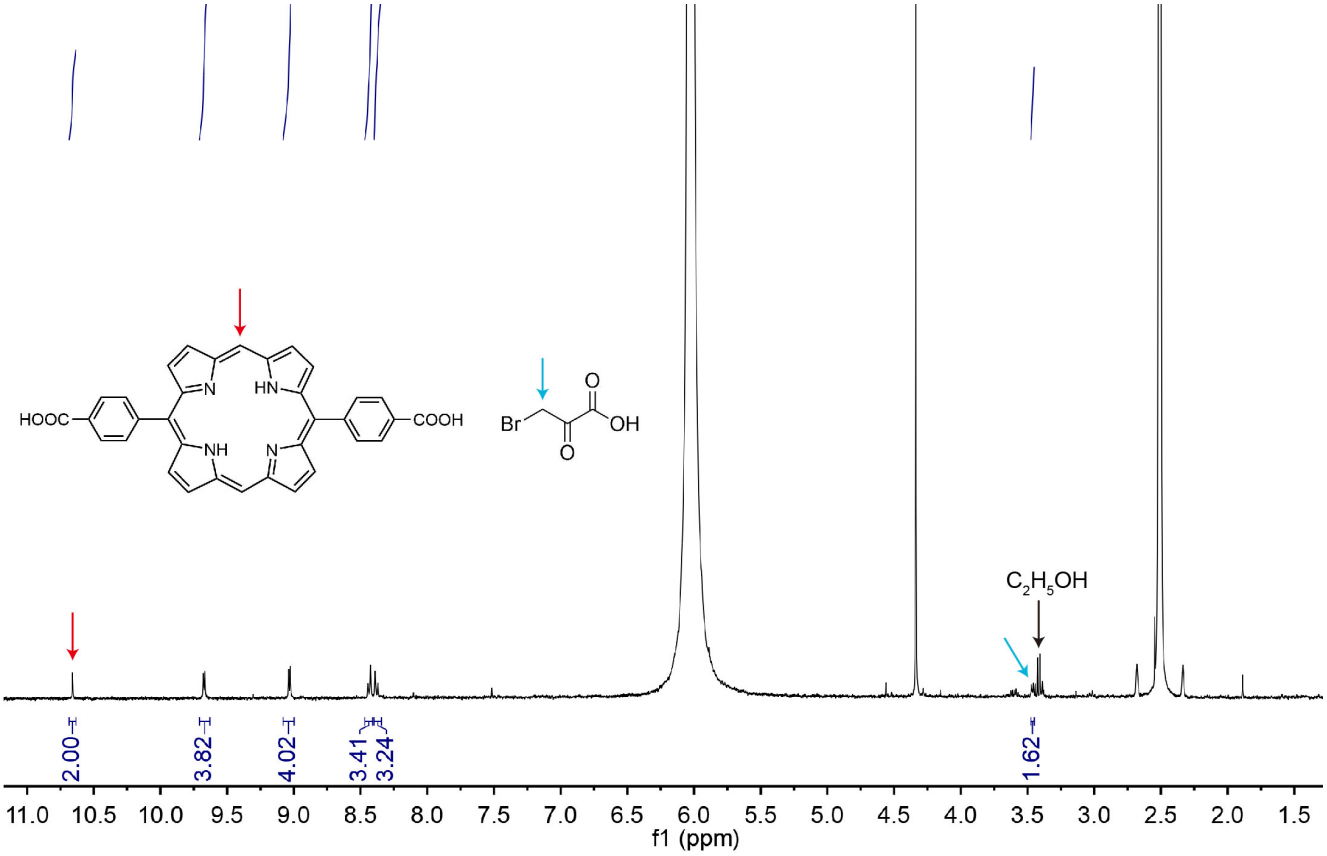

Figure S5. ^{1}H NMR of digested BrP@Hf-DBP MOL.

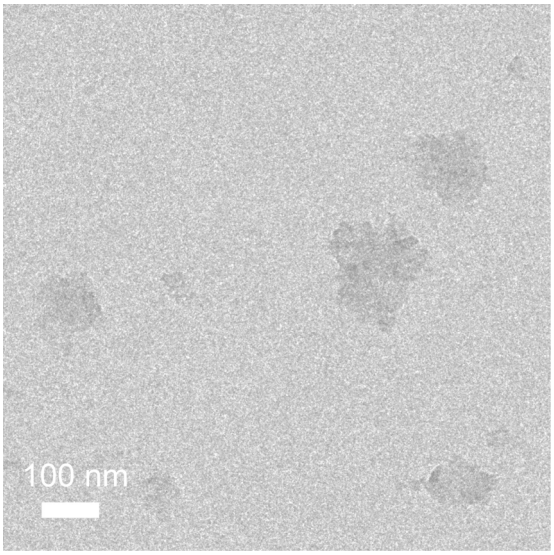

Figure S6. TEM images of TFA-modified Hf-DBP MOL.

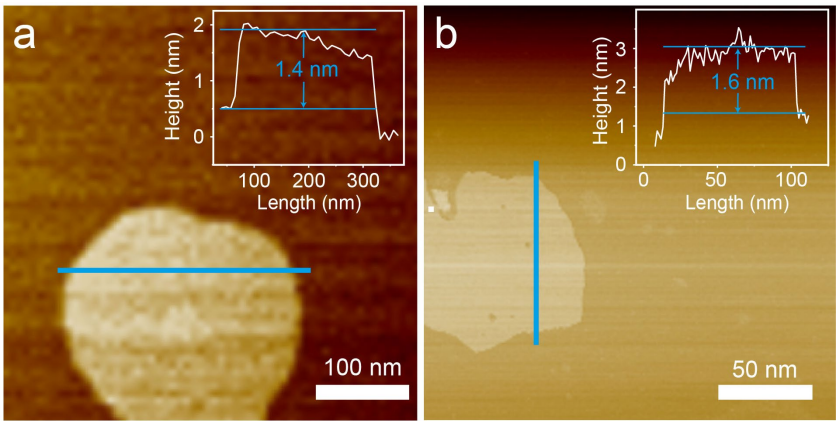

Figure S7. Atomic force microscopy imaging of (a) TFA-modified Hf-DBP MOL and (b) BrP@MOL.

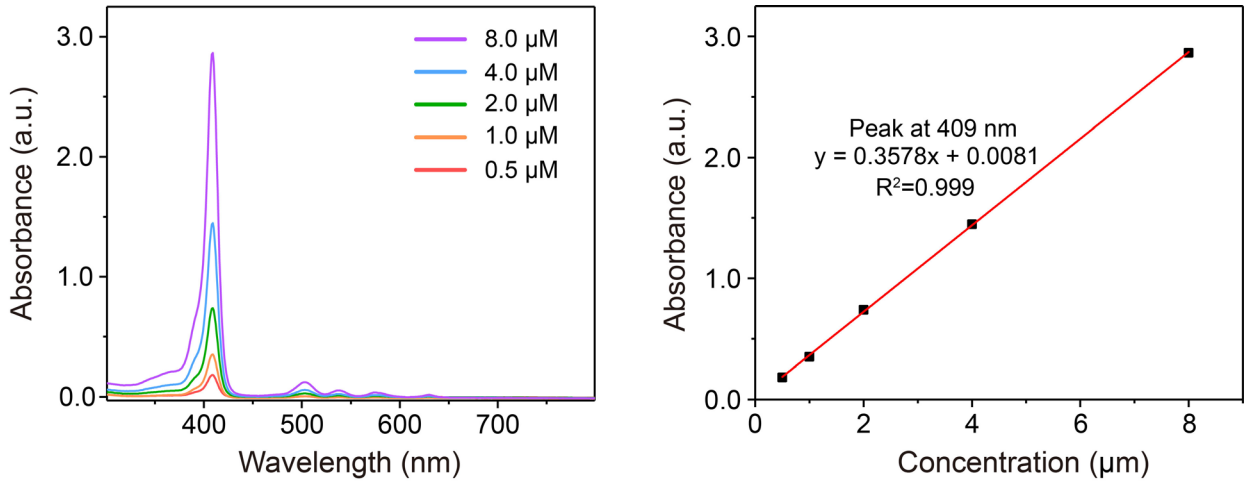

Figure S8. (a) UV-Vis absorption spectra of H_2DBP with different concentrations in DMSO containing 5% H_3PO_4. (b) Linear fitting of the H_2DBP absorbance at 409 nm as a function of concentration.

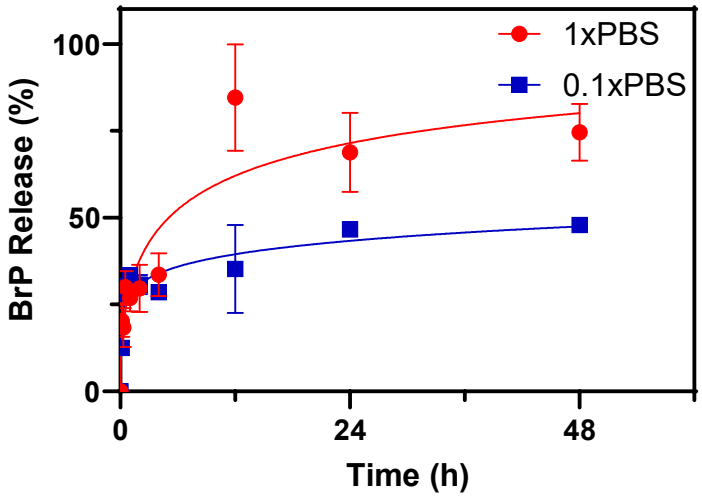

Figure S9. Release percentages of BrP from BrP@MOL after incubation in 1× PBS and 0.1× PBS for 2 days. Data are presented as mean ± SD.

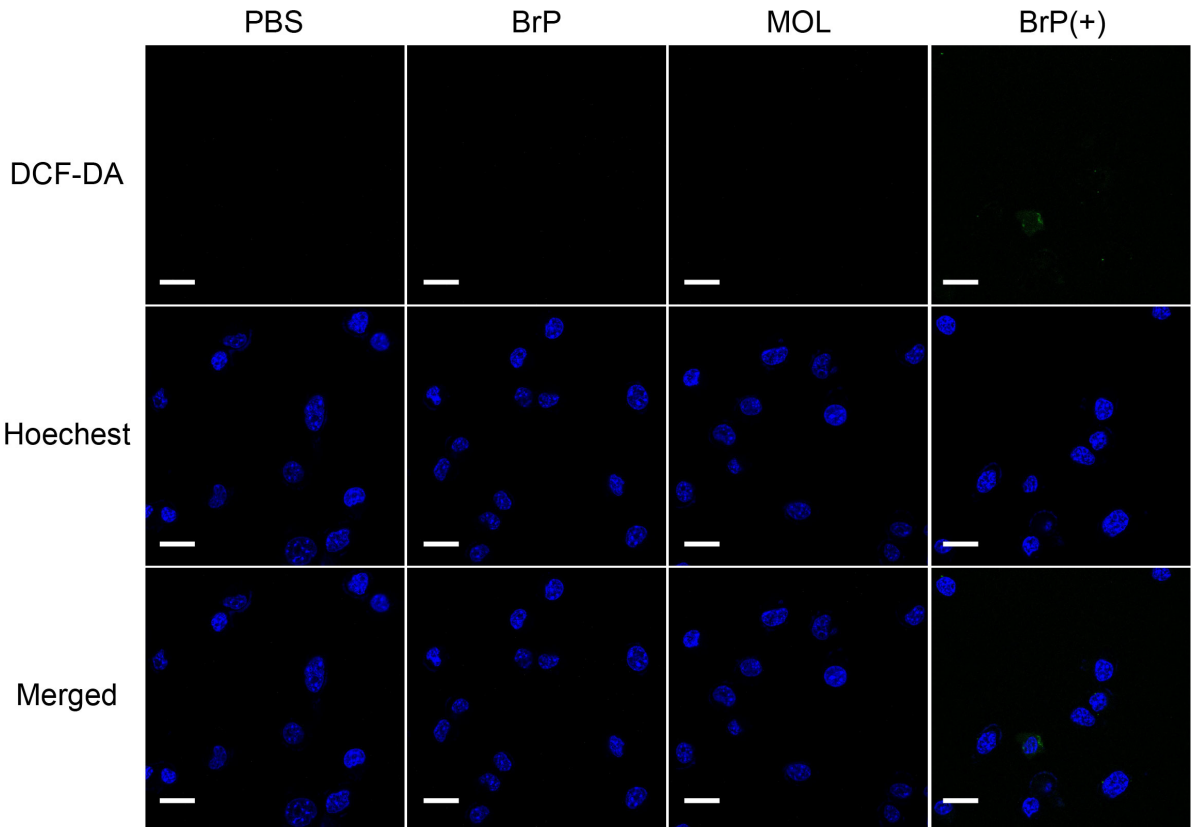

Figure S10. CLSM of ROS generation in CT26 cells after different treatments (DCF-DA, green; Hoechst, blue; scale bar = 20 μm).

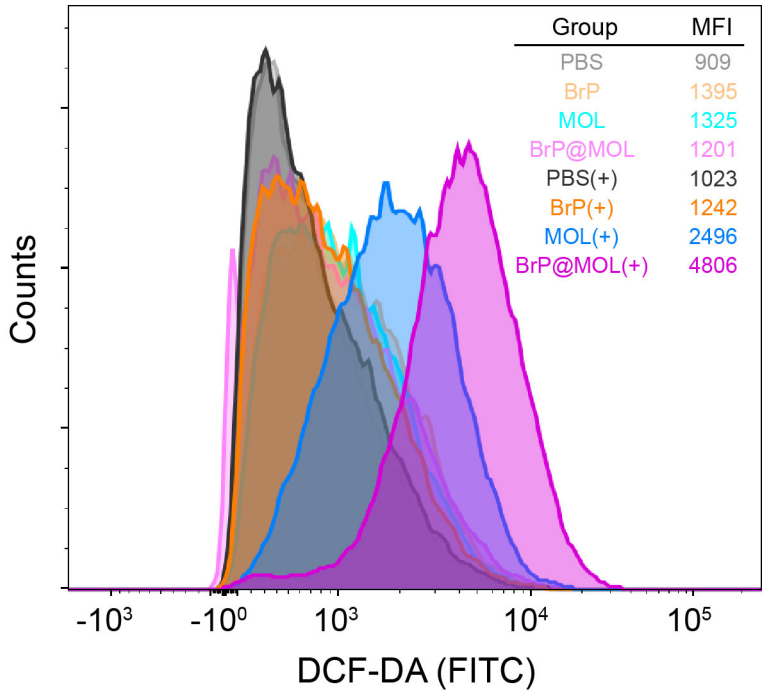

Figure S11. Intracellular ROS generation in CT26 cells after different treatments, determined by flow cytometry.

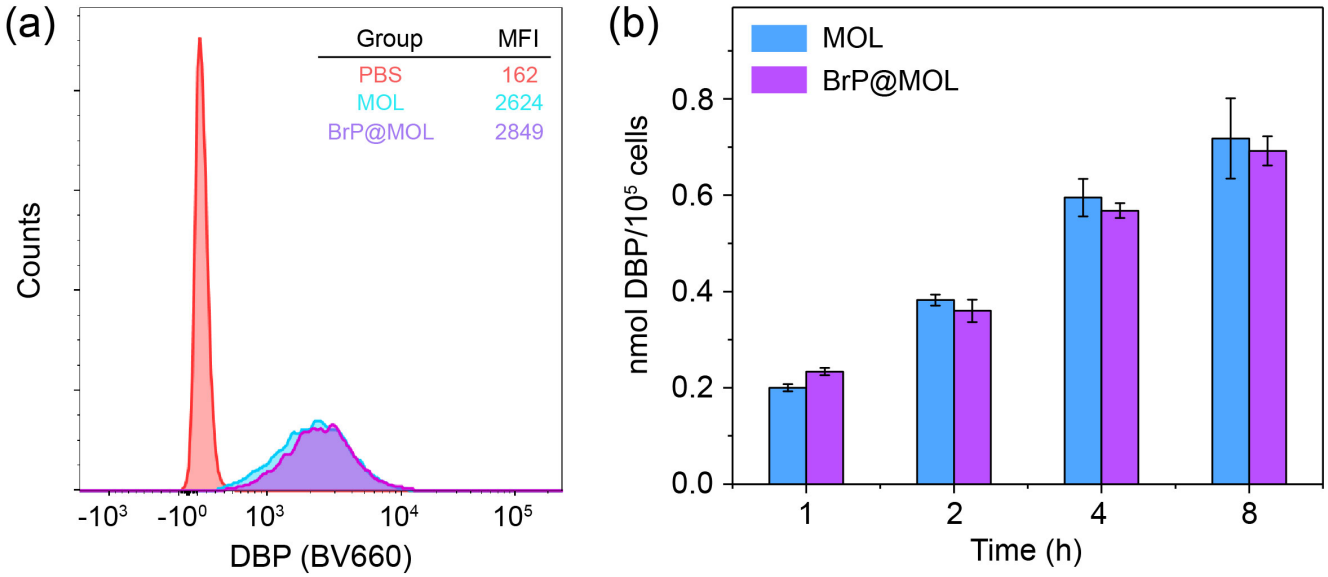

Figure S12. (a) Relative intracellular uptake of MOL and BrP@MOL in CT26 cells after 6 h incubation, determined by flow cytometry. The fluorescence intensity of DBP was measured using the channel of Brilliant Violet 660 (ex 405 nm/em 645 nm). (b) Time-dependent intracellular uptake of MOL or BrP@MOL at different time points determined by UV-Vis spectroscopy. n=3. Data are presented as mean ± SD.

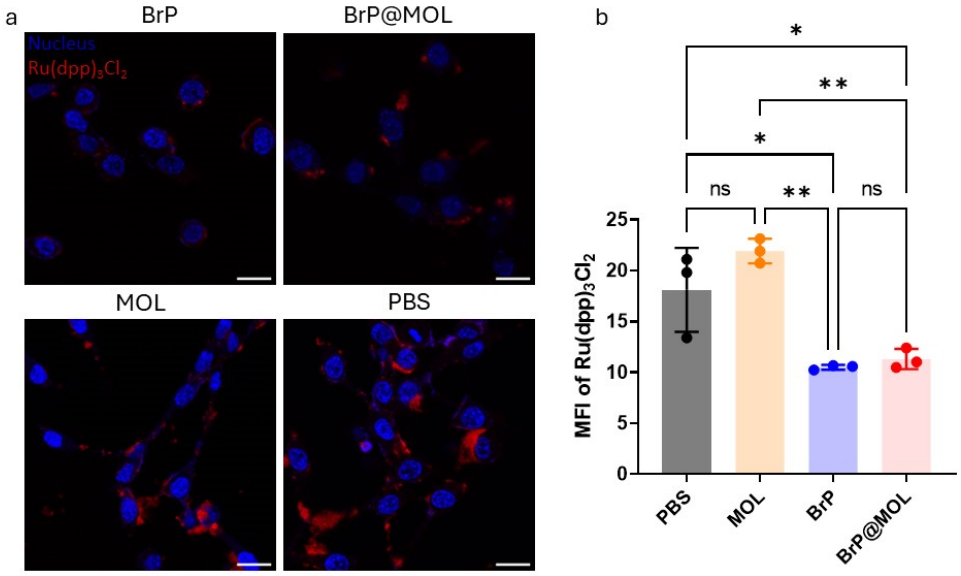

Figure S13. (a) CLSM of $Ru(dpp)_3Cl_2$ in CT26 cells after different treatments (scale bar = 20μm). (b) mean fluorescence intensity (MFI) of $Ru(dpp)_3Cl_2$ in CT26 cells after different treatments as analyzed by CLSM and Fiji ImageJ (NIH). n=3. Data are presented as mean ± SD.

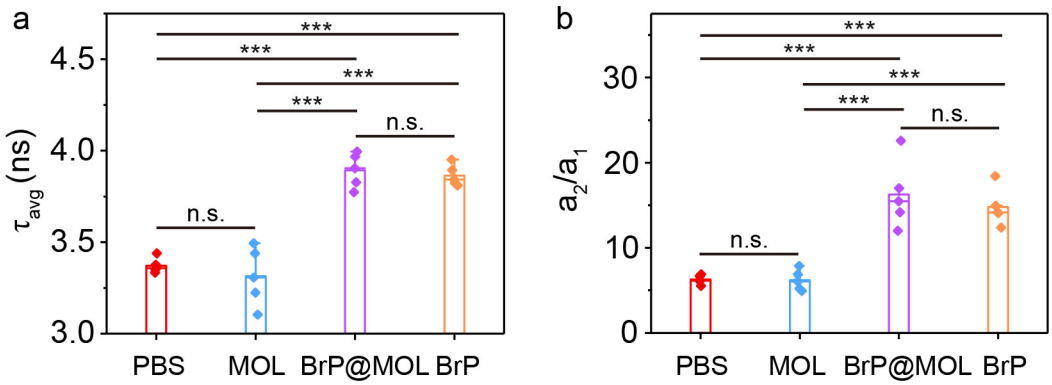

Figure S14. (a) Average fluorescence lifetime (τ_{avg}) of FAD in CT26 cells treated with PBS, MOL, BrP@MOL, or BrP. (b) Free/bound FAD ratio (a_2/a_1) in CT26 cells treated with PBS, MOL, BrP@MOL, or BrP. n=5. Data are presented as mean ± SD.

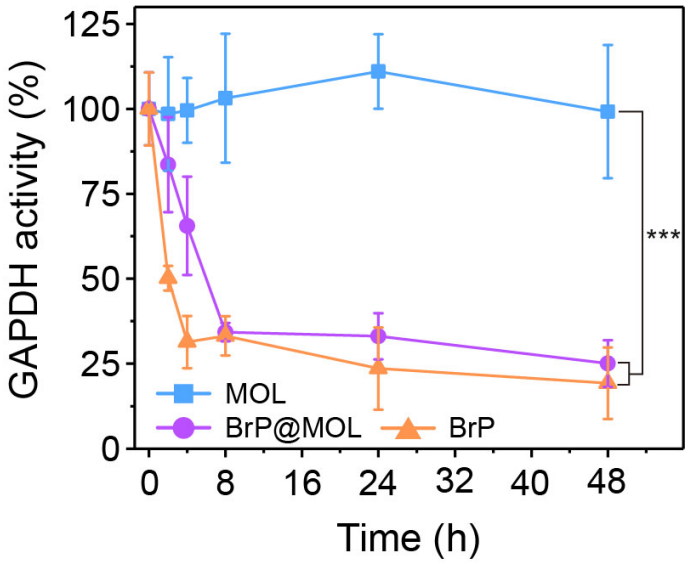

Figure S15. Time-dependent GAPDH activity of CT26 cells treated with MOL, BrP@MOL, or BrP. CT26 cells treated with PBS served as a control. n=3. Data are presented as mean ± SD.

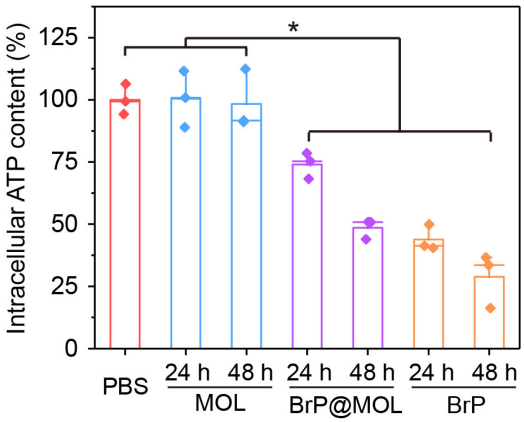

Figure S16. Intracellular ATP in CT26 cells treated with PBS, MOL, BrP@MOL, or BrP. n=3. Data are presented as mean ± SD.

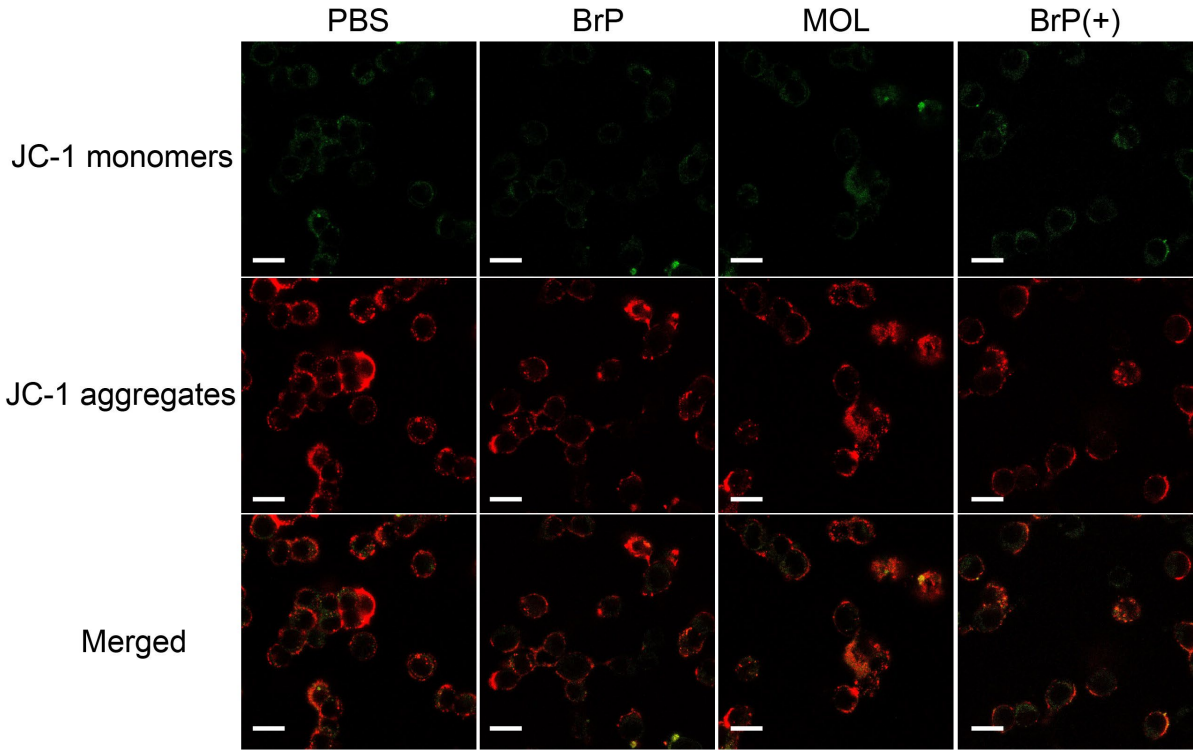

Figure S17. CLSM images of mitochondrial membrane potential in CT26 cells after different treatments (JC-1 monomers, green; JC-1 aggregates, red; scale bar = 20 μm).

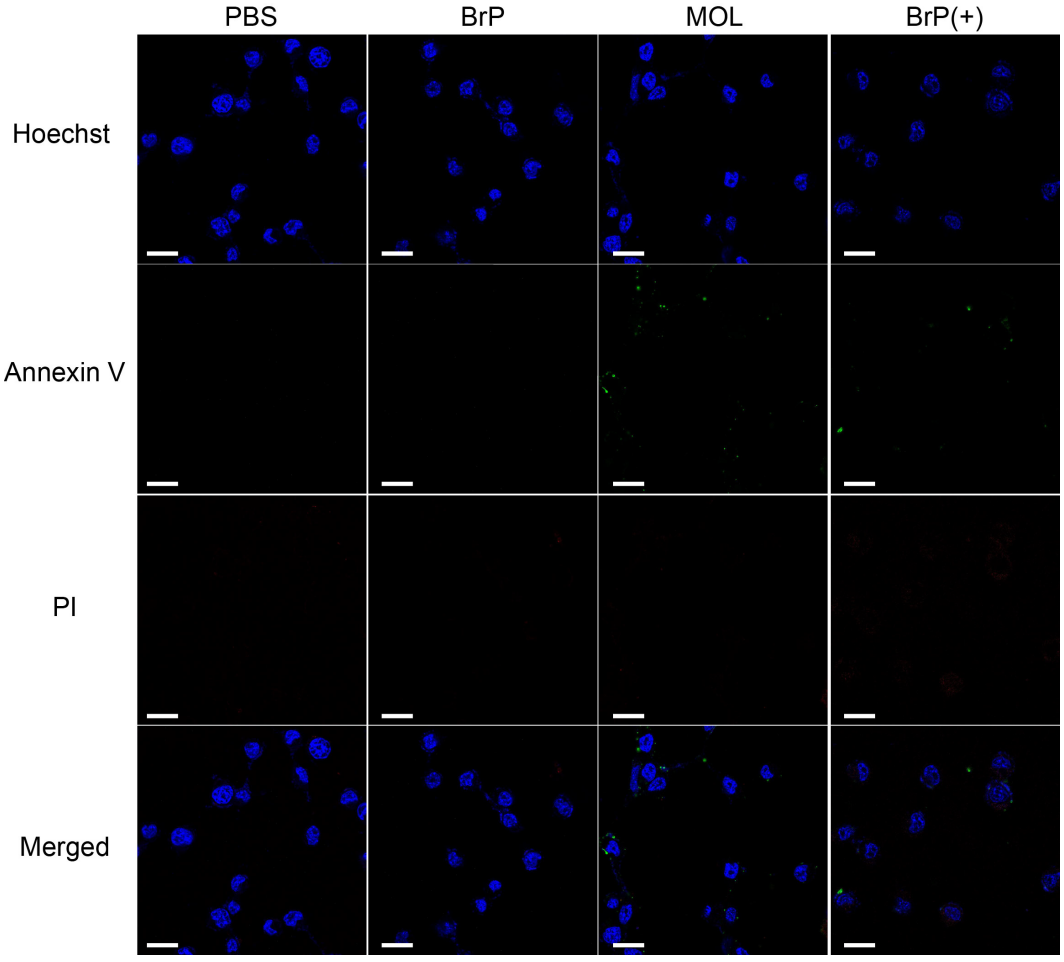

Figure S18. CLSM images of CT26 cell apoptosis after different treatments (Annexin V, green; PI, red; Hoechst, blue; scale bar = 20 μm).

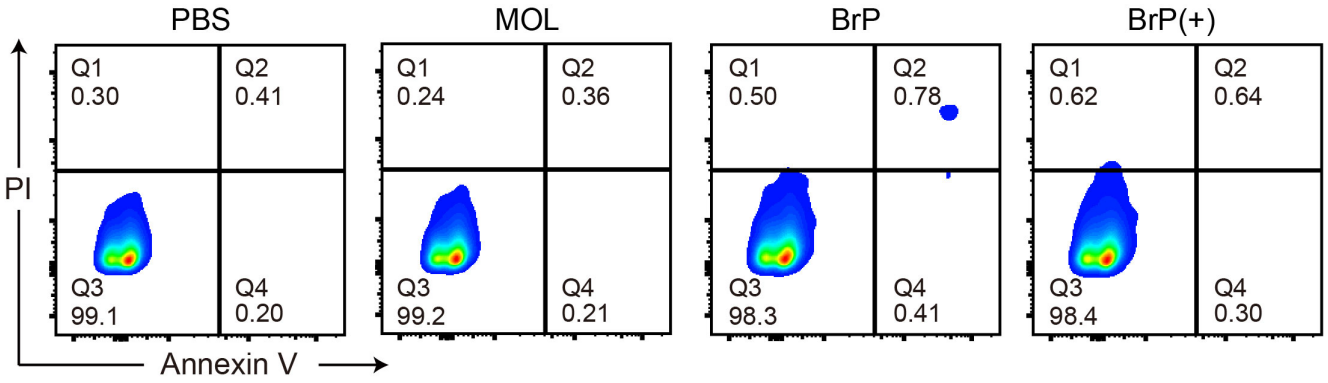

Figure S19. Flow cytometric analysis of Annexin V/PI staining of CT26 after different treatments.

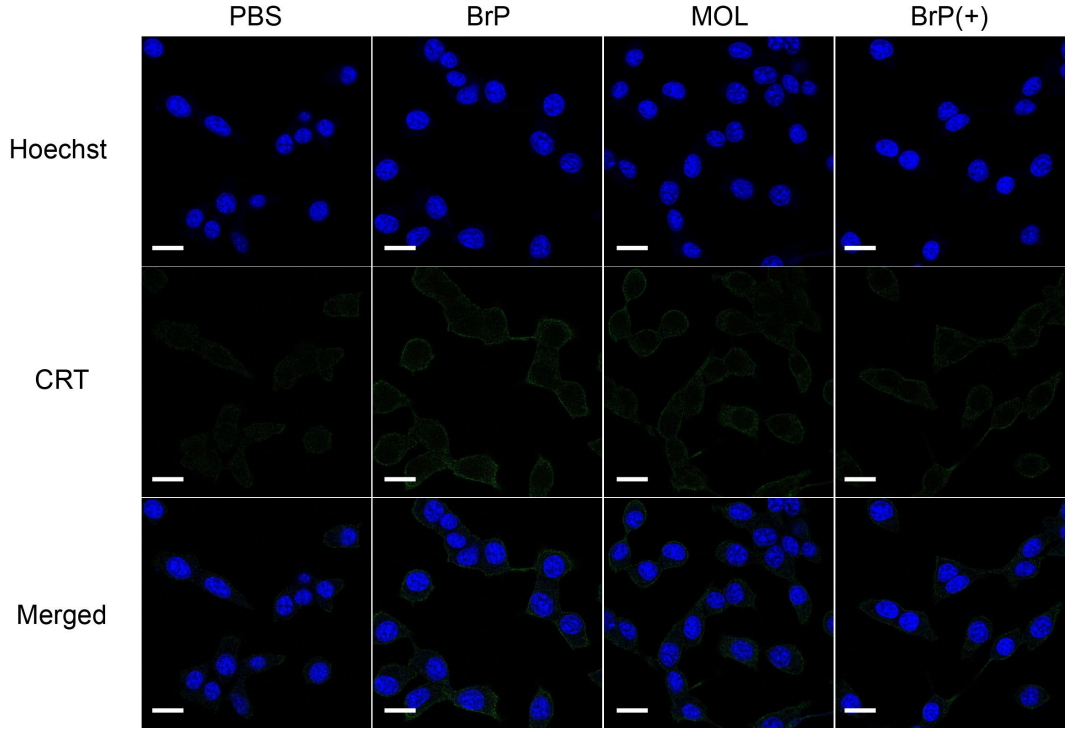

Figure S20. CLSM images of CRT translocation on CT26 cells after different treatments (CRT, green; Hoechst, blue; scale bar = 20 μm).

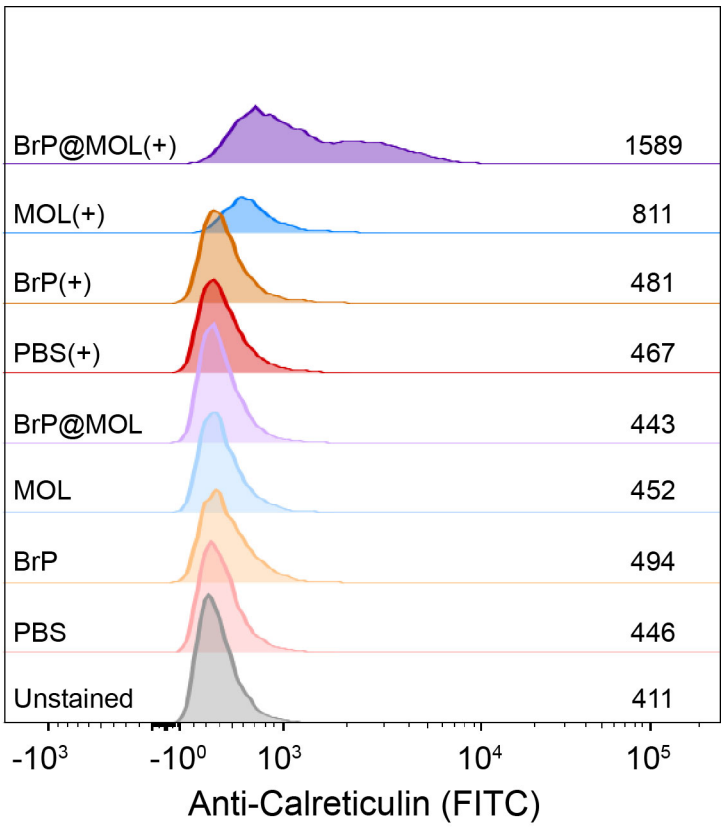

Figure S21. CRT expression on CT26 cells after different treatments, determined by flow cytometry.

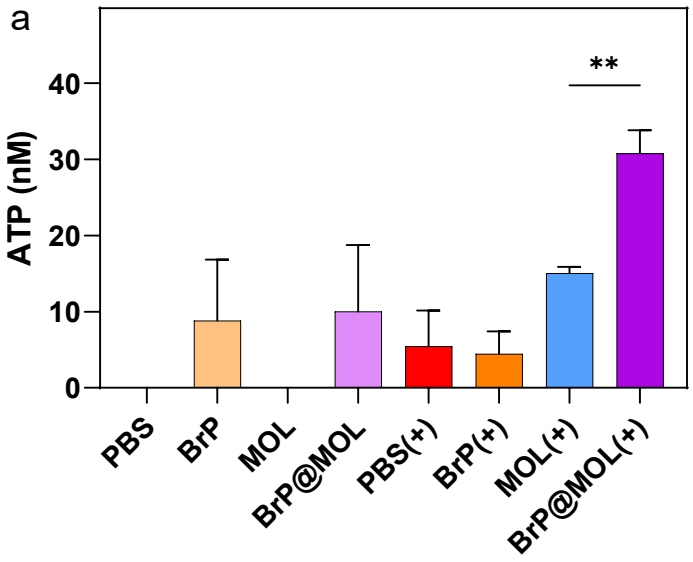

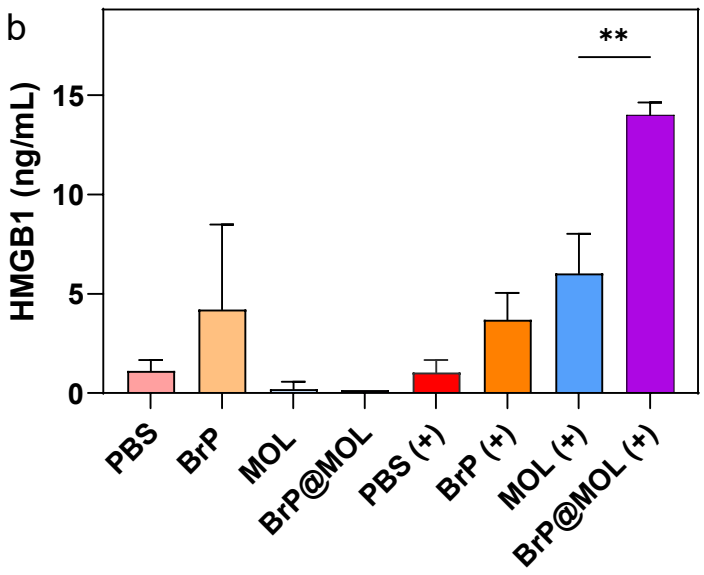

Figure S22. Extracellular ATP (a) and HMGB1 (b) concentrations of CT26 cells at 24 hours post different treatments (n=3). Data are presented as mean ± SD.

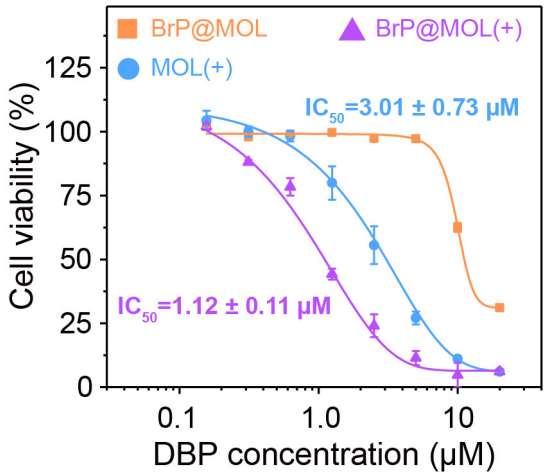

Figure S23. Cell viability of 4T1 cancer cells treated with BrP@MOL(-), MOL(+), or BrP@MOL(+). n=3.

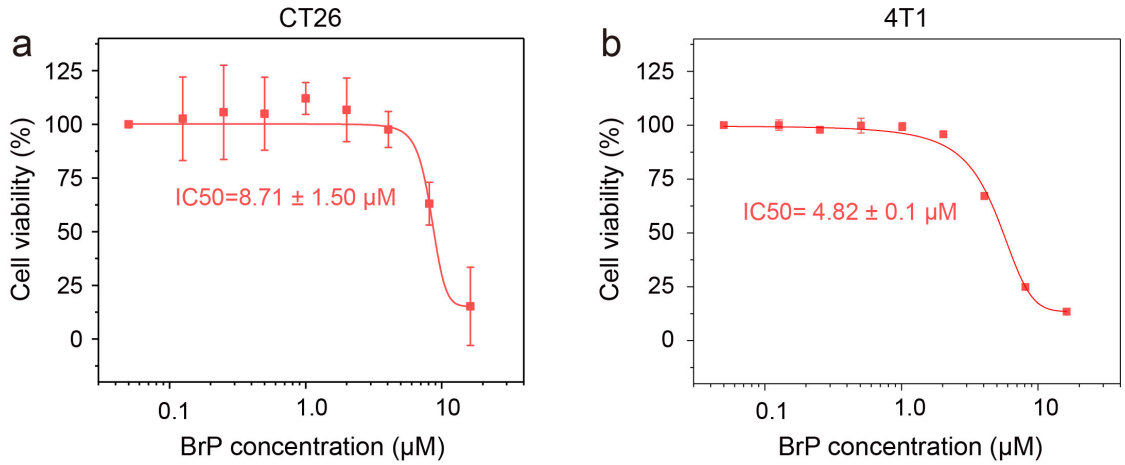

Figure S24. Cell viabilities of CT26 (a) and 4T1 (b) cancer cells treated with BrP. n=3. Data are presented as mean ± SD.

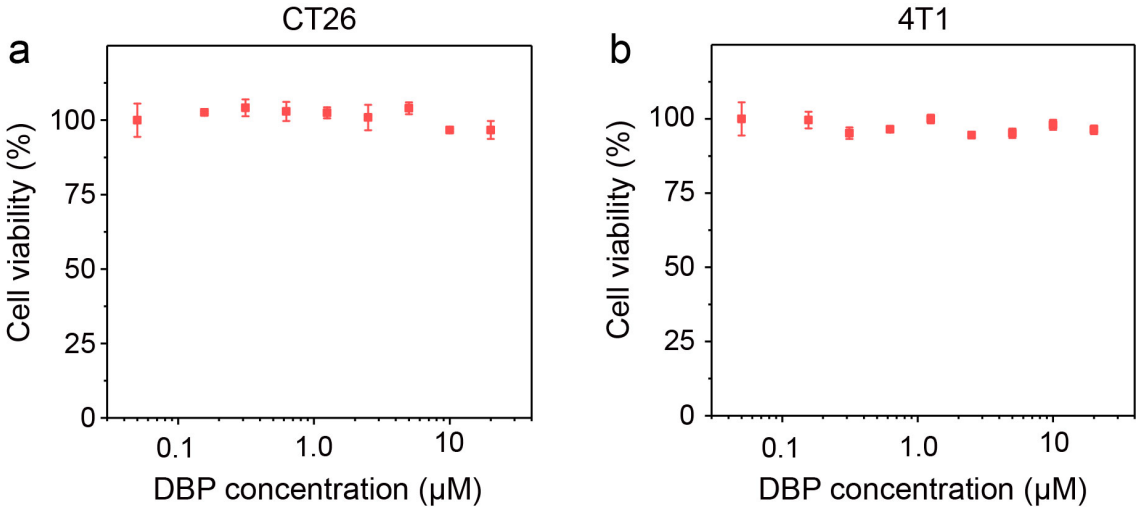

Figure S25. Cell viabilities of CT26 (a) and 4T1 (b) cancer cells treated with MOL. n=3. Data are presented as mean ± SD.

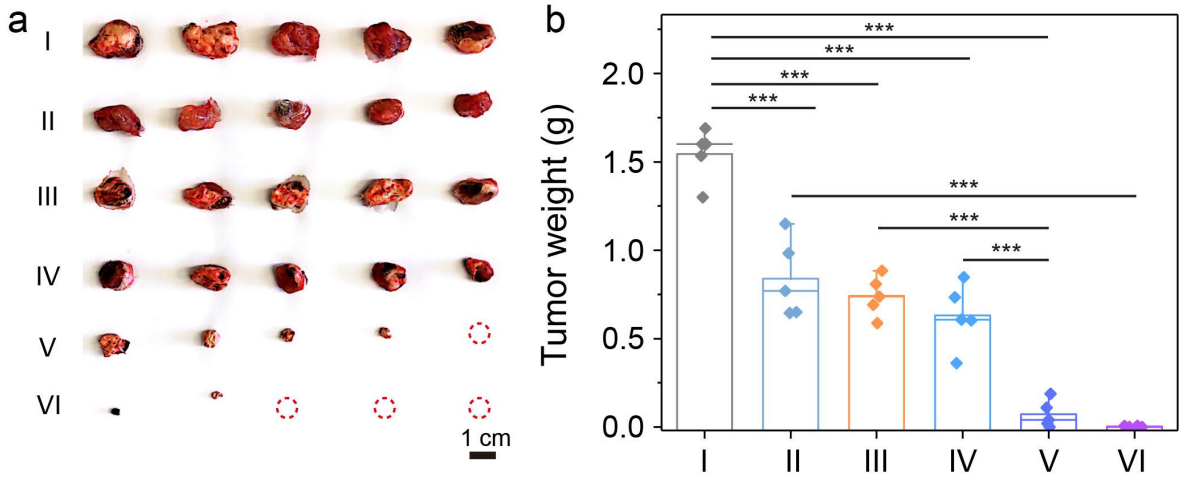

Figure S26. (a) Photograph of excised 4T1 tumors after different treatments (n=5). (b) Weights of excised 4T1 tumors from BALB/c mice after different treatments. I: PBS, II: αPD-L1, III: BrP@MOL, IV: MOL(+), V: BrP@MOL(+), or VI: BrP@MOL(+) + αPD-L1. n=5. Data are presented as mean ± SD. Scale bar = 1.0 cm in a.

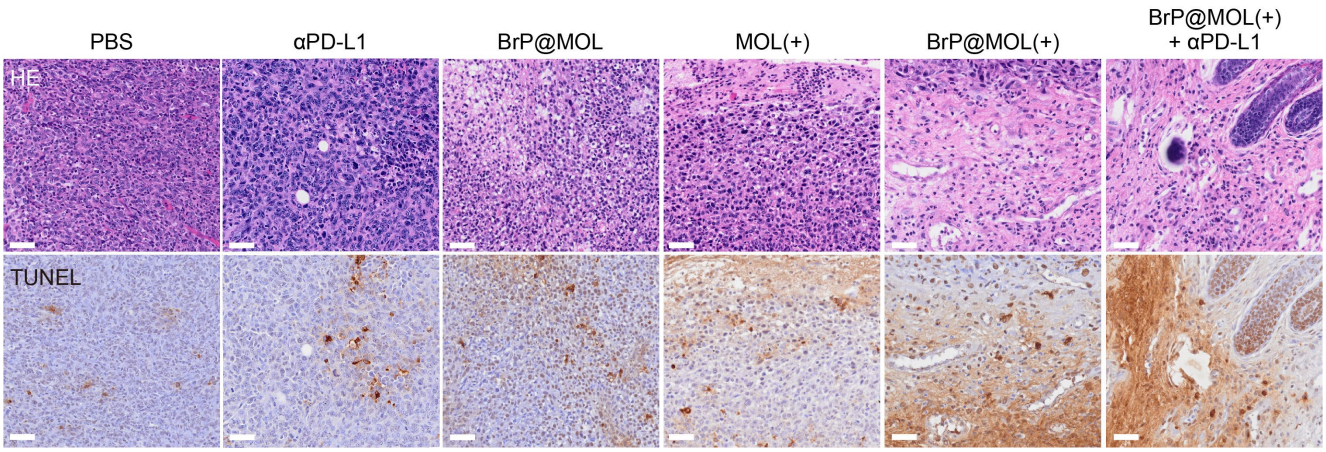

Figure S27. H&E and TUNEL staining of 4T1 tumors after different treatments. Scale bars: 50 μm.

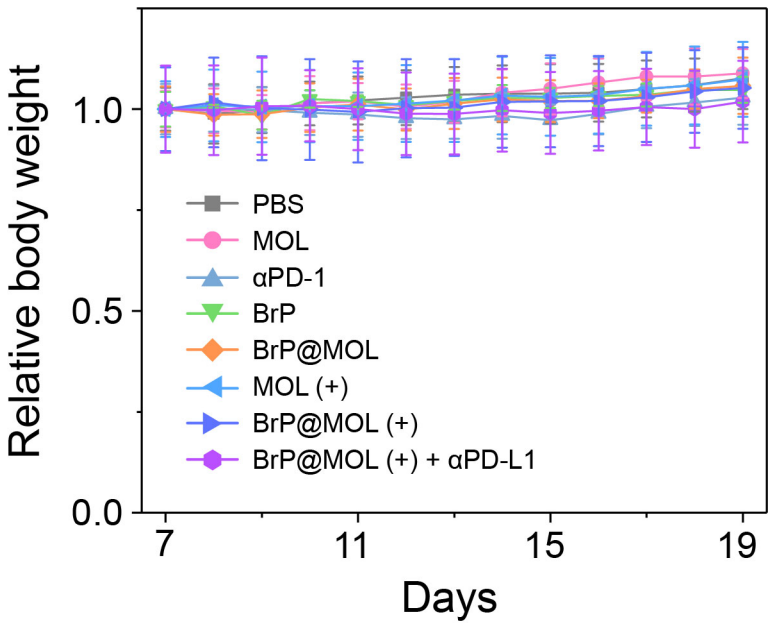

Figure S28. Relative body weight curves of subcutaneous CT26 tumor-bearing BALB/c mice after different treatments. n=5. Data are presented as mean ± SD.

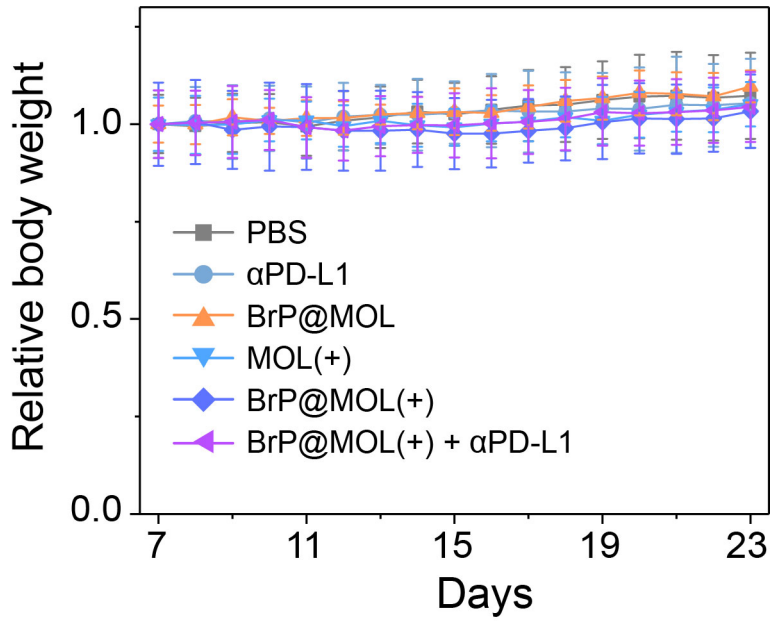

Figure S29. Relative body weight curves of orthotopic 4T1 tumor-bearing BALB/c mice after different treatments. n=5. Data are presented as mean ± SD.

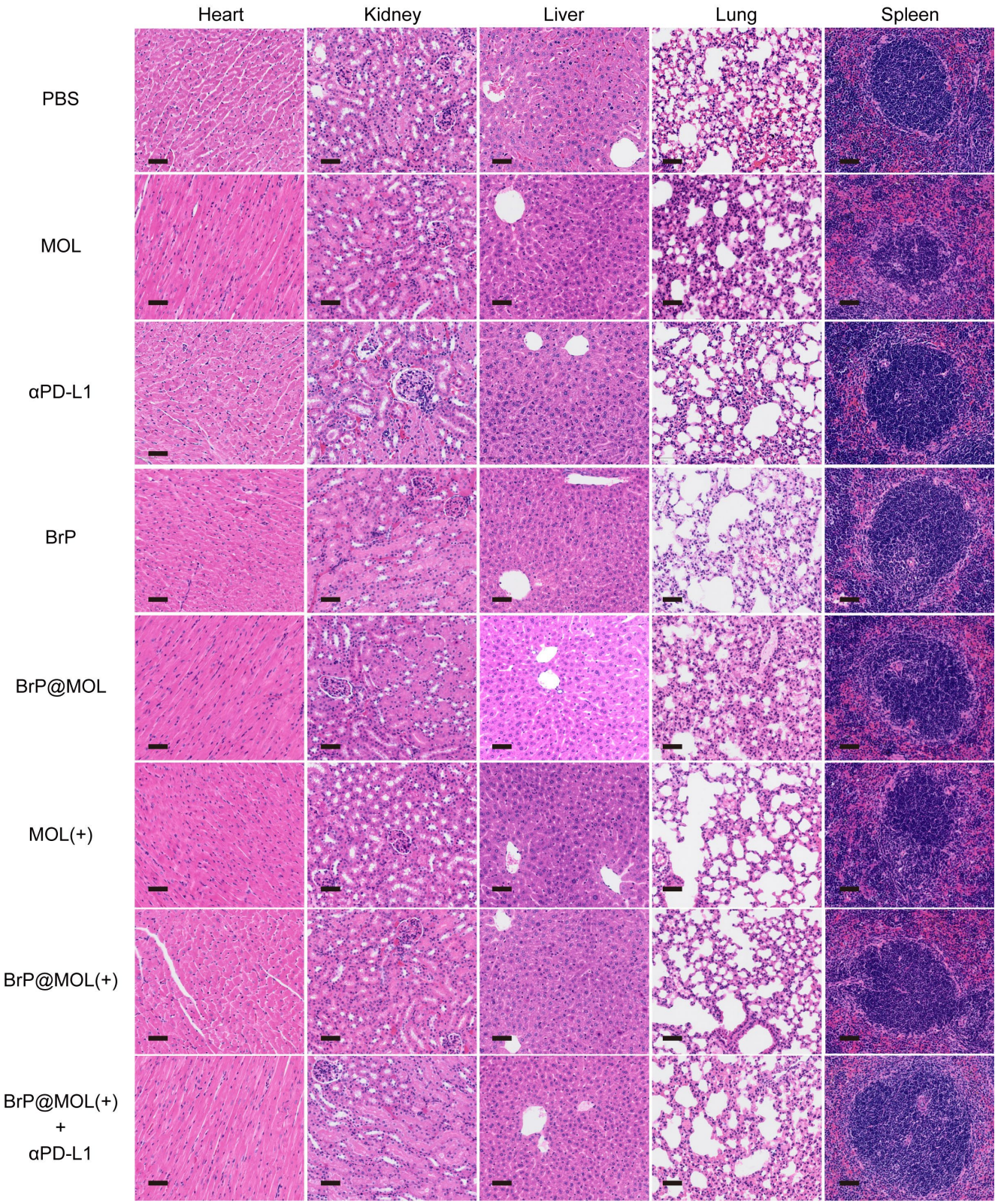

Figure S30. H&E staining of major organs from subcutaneous CT26 tumor-bearing mice. Scale bar = 50 μm.

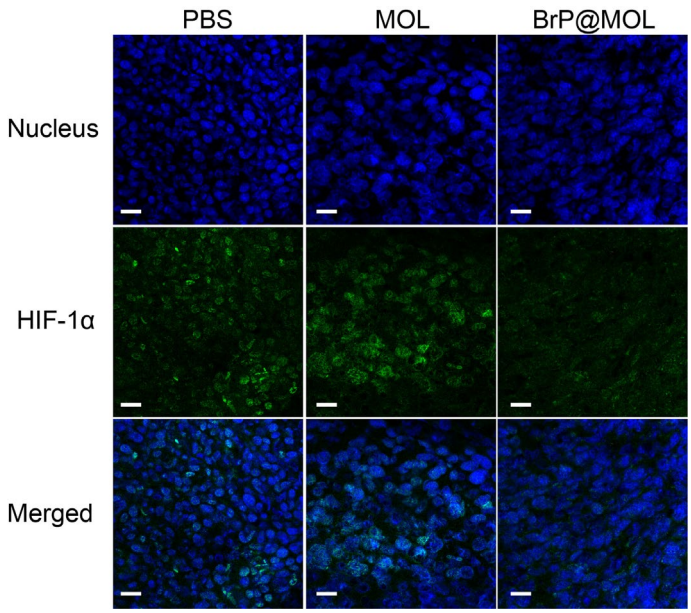

Figure S31. Immunofluorescence staining of hypoxia-inducible factor 1-alpha (HIF-1α) in CT26 tumors treated with PBS, MOL, or BrP@MOL. Scale bars: 20 μm.

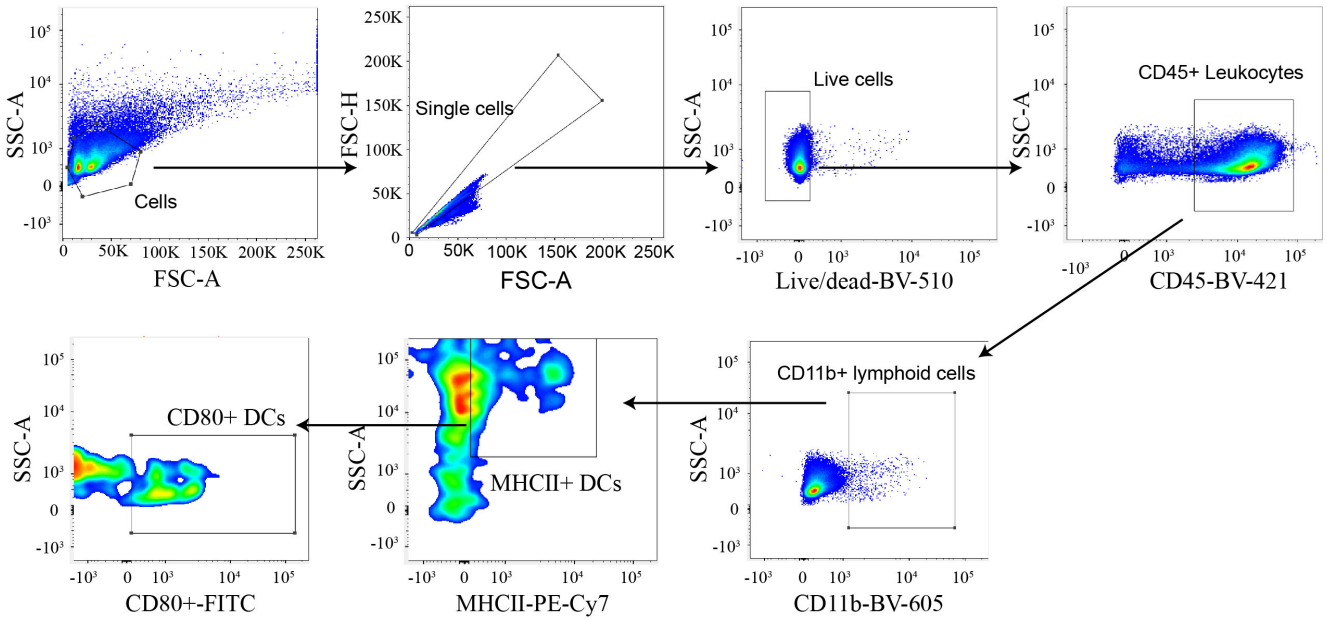

Figure S32. Gating strategies for CD80+ DC (CD45+ CD11b+ MHCII+ CD8+) in Figure 6.

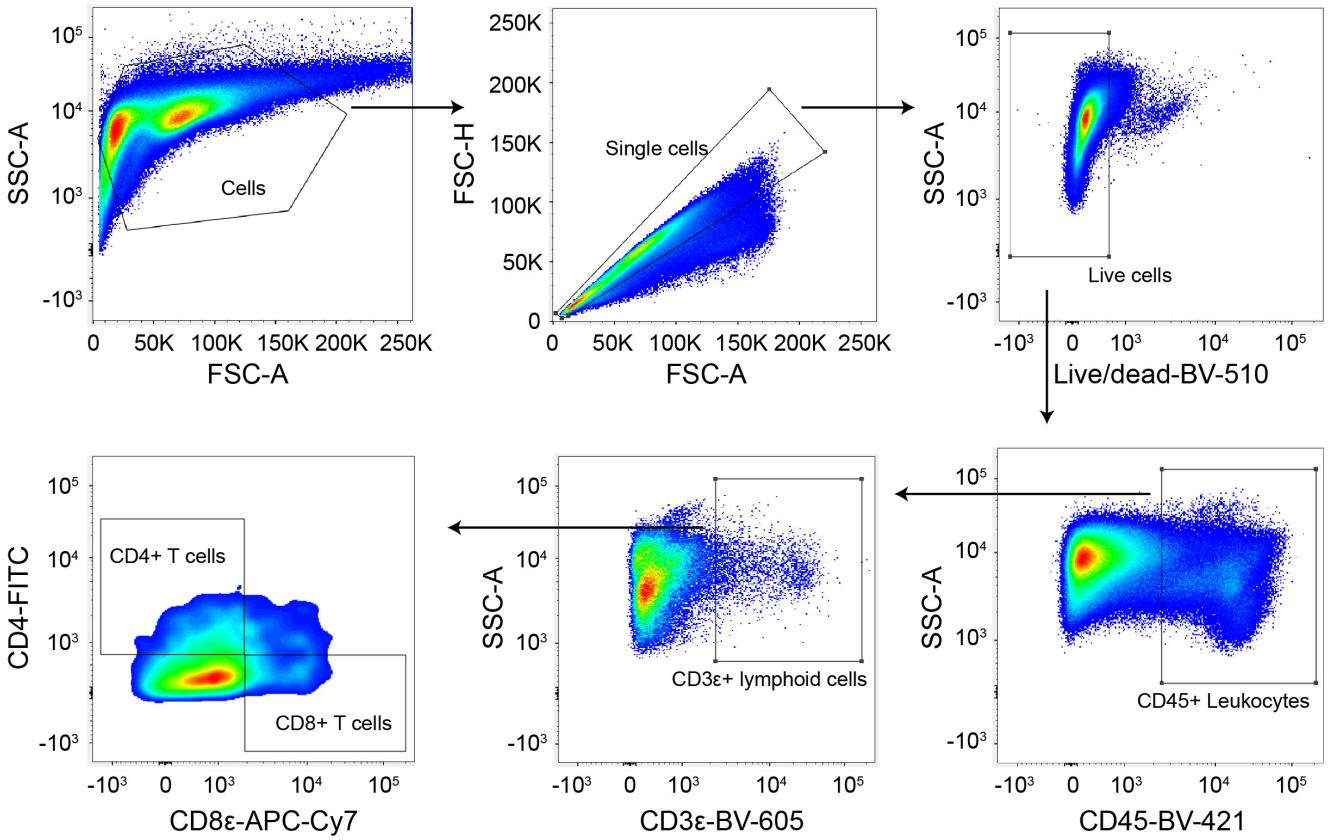

Figure S33. Gating strategies for CD8+ T cells (CD45+ CD3ε CD8+) in Figure 6.

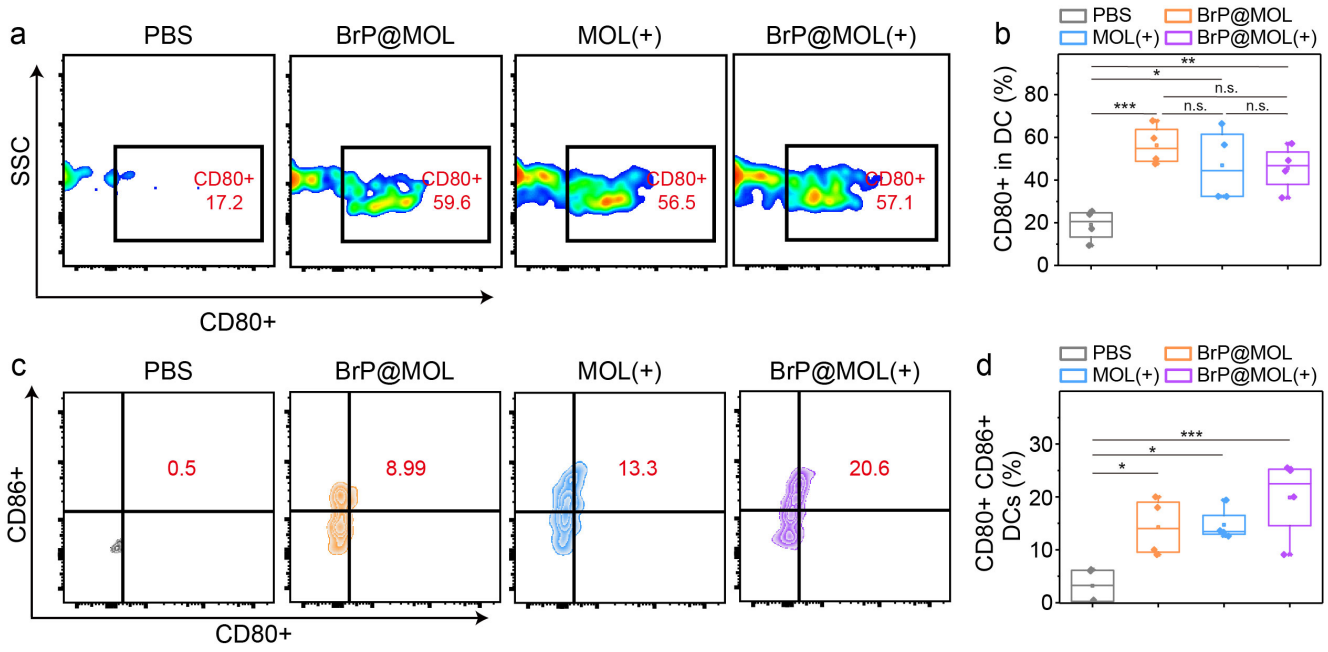

Figure S34. Flow cytometry plots (a) and quantification (b) of CD80+ DCs in the TDLNs from CT26-tumor-bearing mice. Flow cytometry plots (c) and quantification (d) of CD80+CD86 DCs in the TDLNs from CT26-tumor-bearing mice. n=4. Data are presented as mean ± SD. *, $p < 0.05$; **, $p < 0.01$; ***, $p < 0.001$.

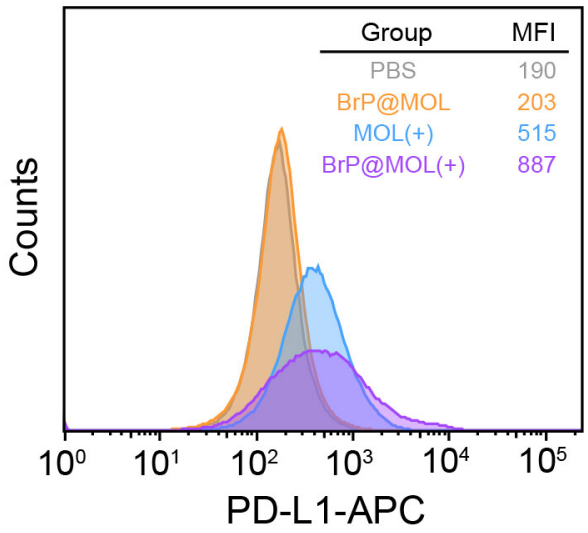

Figure S35. PD-L1 expression in tumor tissues after different treatments.

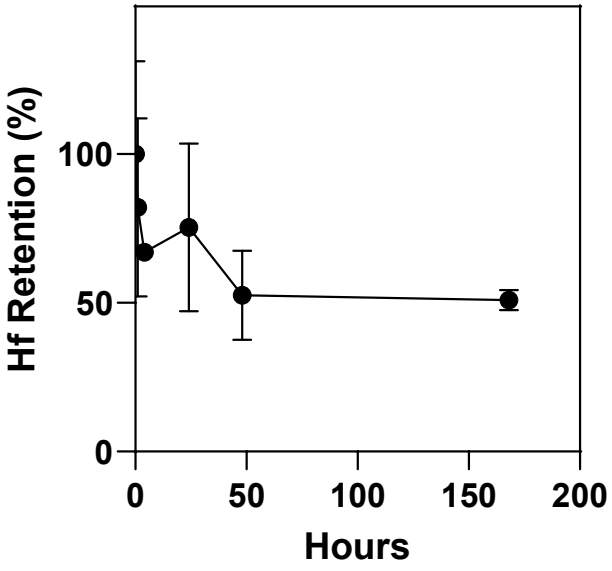

Figure S36. Tumor retention of BrP@MOL as measured by Hf ICP-MS (n=3). Data are presented as mean ± SD.

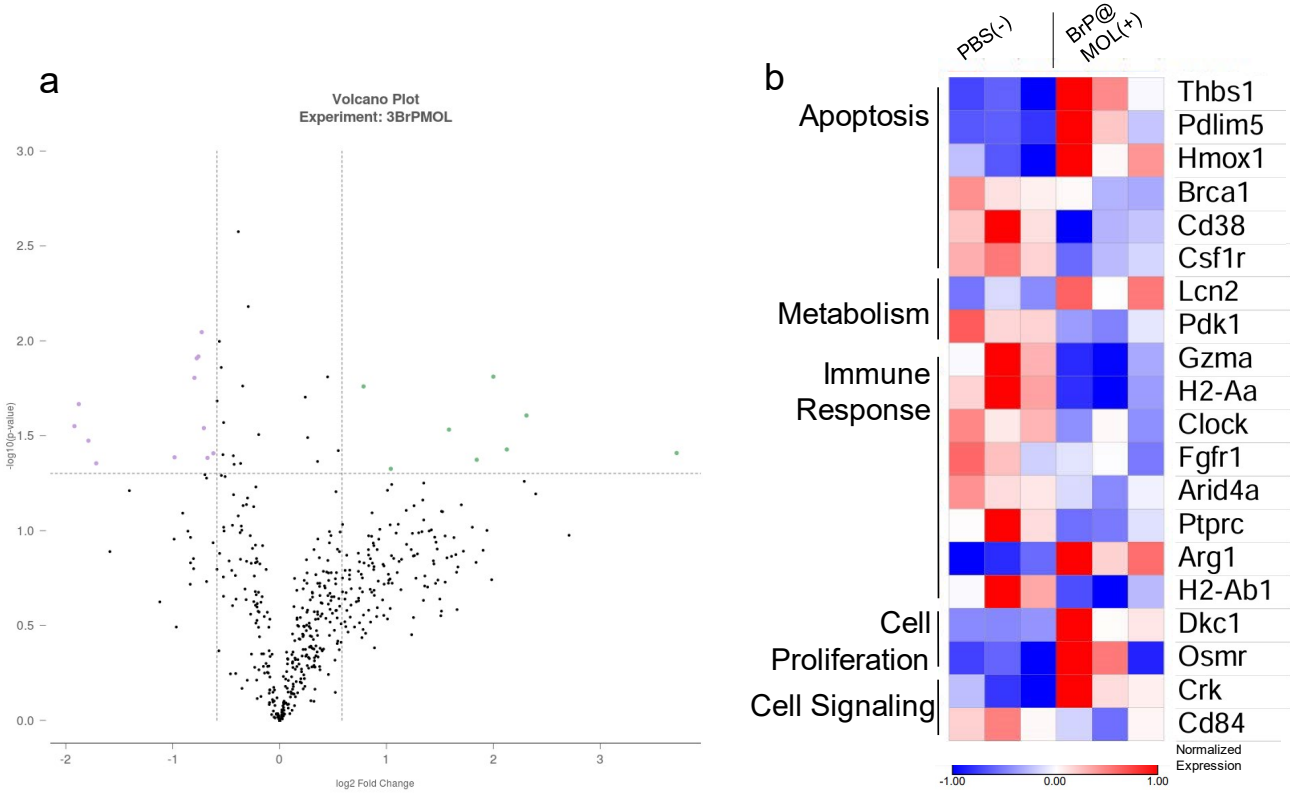

Figure S37. Differential expression of genes in bulk tumors 7 days after BrP@MOL(+) or PBS treatment from nanoString analysis.

Table S1. IC_{50} values of BrP@MOL and MOL with or without light irradiation on CT26 cells.

	BrP@MOL	MOL
With light	0.50 ±0.15μM	2.00 ± 0.20 μM
Without light	> 20 μM	> 20 μM

Table S2. IC_{50} values of BrP@MOL and MOL with or without light irradiation on 4T1 cells.

	BrP@MOL	MOL
With light	1.12 ± 0.11 μM	3.01 ± 0.73 μM
Without light	9.8 ± 0.27 μM	> 20 μM

Table S3. Calculated $f_{additive}$ and $f_{combination}$ values for CT26 cells

cDBP (μM)	$f_{additive}$	$f_{combination}$
0.3125	0.93	0.707
0.625	0.796	0.49
1.25	0.581	0.267
2.5	0.420	0.104
5.0	0.177	0.116
10.0	0.126	0.046

Table S4. Calculated $f_{additive}$ and $f_{combination}$ values for 4T1 cells

cDBP (μM)	$f_{additive}$	$f_{combination}$
0.3125	0.979	0.881
0.625	0.971	0.784
1.25	0.796	0.442
2.5	0.54	0.24
5.0	0.262	0.114
10.0	0.069	0.047

Table S5. Tumor growth inhibition (TGI) values for CT26 tumor model at the endpoint.

Group	TGI
PBS(-)	0%
MOL(-)	4.2%
BrP(-)	46.8%
BrP@MOL(-)	47.6%
MOL(+)	65.0%
BrP@MOL(+)	93.6%
BrP@MOL(+) + α-PD-L1	99.1%

Table S6. Tumor growth inhibition (TGI) values for 4T1 tumor model at the endpoint.

Group	TGI
PBS(-)	0 %
BrP@MOL(-)	41.9%
MOL(+)	56.0%
BrP@MOL(+)	91.4%
BrP@MOL(+) + α-PD-L1	98.5%

4. References

(1) Luo, T.; Fan, Y.; Mao, J.; Yuan, E.; You, E.; Xu, Z.; Lin, W. *Journal of the American Chemical Society* **2022**, *144*, 5241.

(2) Liu, H.; Zhang, Q.; Huang, H.; Qiu, M.; Hu, L.; Zhao, X.; Xu, C.; Wang, Z.; Zhang, C.; Zhan, Y.; Sun, Y. *Biomedical Chromatography* **2022**, 36(12), 5477.